

REON
SACRAMENTO PLANT



REPORT NO. RN-S-0274

TO

AEC - NASA SPACE NUCLEAR PROPULSION OFFICE

DESIGN EQUATION ANALYSIS FOR HEAT TRANSFER TO
CRYOGENIC HYDROGEN AT PRESSURES FROM 600 TO 1500 PSIA
AND WALL-TO-BULK TEMPERATURE RATIOS TO 20

JUNE 1966

NERVA PROGRAM

CONTRACT SNP-1

FACILITY FORM 602

N67-34804

(ACCESSION NUMBER)

(THRU)

65
(PAGES)

1
(CODE)

CR-87511
(NASA CR OR TMX OR AD NUMBER)

23
(CATEGORY)



AEROJET-GENERAL CORPORATION

SACRAMENTO, CALIFORNIA



REPORT NO. RN-S-0274

DESIGN EQUATION ANALYSIS FOR HEAT TRANSFER TO
CRYOGENIC HYDROGEN AT PRESSURES FROM 600 TO 1500 PSIA
AND WALL-TO-BULK TEMPERATURE RATIOS TO 20

JUNE 1966



ROCKET ENGINE OPERATIONS - NUCLEAR

NERVA PROGRAM

CONTRACT SNP-1

CLASSIFICATION CATEGORY

UNCLASSIFIED

WR Thompson
CLASSIFYING OFFICER

6-6-66
DATE

AEROJET-GENERAL CORPORATION
A SUBSIDIARY OF THE GENERAL TIRE & RUBBER COMPANY

PRECEDING PAGE BLANK NOT FILMED.

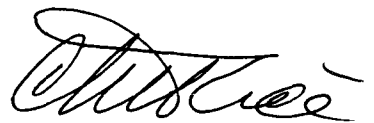
ABSTRACT

Experimental single-tube heat-transfer data from all available sources have been analyzed in terms of various design equations in an effort to select that model which best represents the data. Cryogenic hydrogen data so analyzed were restricted to the pressure range from 600 to 1500 psia and to wall-to-bulk temperature ratios to 20.

A graphical presentation of the ratio of the experimental to the computed heat transfer coefficient as a function of bulk temperature was made for each design equation studied. A lower-limit line was constructed as the locus of the high-density data point concentration; the nominal design equation was then established so that the lower limit line was 80% of the nominal equation. The level of confidence for each modified equation was then based on the percentage of data points located within the $\pm 20\%$ limits to the nominal lines. From these plots a variable liquid-side coefficient, C_L , was determined as a function of bulk temperature.

Of the film temperature equations evaluated, that generated by Hess and Kunz appeared to best represent the data; for the equations based on the bulk temperature as reference, the equation known as REON "B" exhibited the least scatter.

The results obtained by incorporating the variable C_L values for both these equations in the analysis of a reactor test of NERVA nozzle S/N-022 were compared with the predictions generated using the nominal design equations. Very little difference in the heat flux profile was found; changes in the coolant bulk temperature and pressure profiles were evident but not of great significance. However, appreciable differences in coolant-side wall temperatures were predicted, up to nearly 200°R just downstream of the nozzle throat. Limited braze alloy data tend to support the selection of the Hess and Kunz equation with variable C_L . A definitive selection of the best predictive equation, however, must await a more direct measurement of tube wall temperature, particularly in the divergent portion of the nozzle.



W. D. Stinnett
Program Manager
REON

for

TABLE OF CONTENTS

	<u>Page</u>
Abstract	iii
Nomenclature	vii
I. Summary	1
II. Introduction	3
III. Experimental Test Programs	7
IV. Correlation of Experimental Test Data	9
A. Computer Regression Analysis	9
B. Graphical Analysis	13
C. Bulk Temperature Correlations	25
D. Film Temperature Correlations	32
E. Effect of System Geometry	37
V. Discussion of Results	43
VI. Conclusions and Recommendations	53
REFERENCES	54

LIST OF FIGURES

	<u>Page</u>
1 Comparison of Experimental and Predicted Heat Transfer Coefficients, LRC Test 667 Data	15
2 Comparison of Experimental and Predicted Heat Transfer Coefficients, LRC Test 708 Data	16
3 Comparison of Experimental and Predicted Heat Transfer Coefficients, LRC Test 881 Data	17
4 REON "A" Equation Predictions in Terms of the Goldmann Heat Flux Parameter and Wall and Bulk Temperatures	19
5 REON "B" Equation Predictions in Terms of the Goldmann Heat Flux Parameter and Wall and Bulk Temperatures	20
6 Modified Film Temperature Equation Predictions in Terms of the Goldmann Parameter and Wall and Bulk Temperatures	21
7 Hess and Kunz Equation Predictions in Terms of the Goldmann Heat Flux Parameter and Wall and Bulk Temperatures	22
8 Nusselt Film Equation Predictions in Terms of the Goldmann Heat Flux Parameter and Wall and Bulk Temperatures	23
9 Experimental/Calculated Heat Transfer Coefficient Ratio Comparison with the REON "A" Equation Prediction	26
10 Experimental/Calculated Heat Transfer Coefficient Ratio Comparison with the REON "B" Equation Prediction	27
11 Experimental/Calculated Heat Transfer Coefficient Ratio Comparison with the McCarthy-Wolf Equation Prediction	28
12 Experimental/Calculated Heat Transfer Coefficient Ratio Comparison with the Dalle Donne-Bowditch Equation Prediction	29
13 Comparison of Bulk Temperature Correlations for Liquid Hydrogen Heat Transfer	30
14 Experimental/Calculated Heat Transfer Coefficient Ratio Comparison with the Hess and Kunz Equation Prediction (Straight Tube Data)	33
15 Experimental/Calculated Heat Transfer Coefficient Ratio Comparison with the AGC Modified Film Temperature Equation Prediction (Straight Tube Data)	34
16 Experimental/Calculated Heat Transfer Coefficient Ratio Comparison with the Nusselt Film Equation Prediction (Straight Tube Data)	35
17 Experimental/Calculated Heat Transfer Coefficient Ratio Comparison with the Miller-Seader-Trebes Equation Prediction (Straight Tube Data)	36
18 Experimental/Calculated Heat Transfer Coefficient Ratio Comparison with the Hess and Kunz Equation Prediction (Curved Tube Data)	38
19 Experimental/Calculated Heat Transfer Coefficient Ratio Comparison with the REON "B" Equation Prediction (Curved Tube Data)	39

List of Figures, (Continued)

		<u>Page</u>
20	Comparison of the "Unswept" Side Heat Transfer Coefficient with that Predicted by the Hess and Kunz Equation	42
21	Coolant-Side Wall Temperature and Heat Flux Profiles for S/N-022 NERVA Nozzle as Predicted by the Nominal Hess and Kunz Design Equation and the Hess-Kunz and the REON "B" Equations with Variable C_L Values	46
22	Coolant Bulk Temperature Profile for S/N-022 NERVA Nozzle as Predicted by the Nominal Hess and Kunz Design Equation and the Hess and Kunz Equation with a Variable C_L	47
23	Coolant-Side Static Pressure Profile for S/N-022 NERVA Nozzle as Predicted by the Nominal Hess and Kunz Design Equation and the Hess-Kunz and the REON "B" Equations with Variable C_L Values	48
24	Predicted and Measured Gas-Side Wall Temperature Profile During Reactor Test NRX-A3	51

List of Tables

		<u>Page</u>
I	Range of Test Parameters	10
II	Coolant-Side Design Equations	11
III	Percentage of Points for h/h_c Ratio Within $\pm 20\%$ of the C_L Design Line on Figures 9-12 and 14-17	45

NOMENCLATURE

$a_1, a_2 \dots a_5$	Terms in Equation (5)
b_w	Factor in Equation (6)
C_L	Liquid-side coefficient multiplier
c_p	Specific heat at constant pressure, Btu/lbm $^{\circ}$ R
D	Inside diameter of tube, in.
f	Flow resistance coefficient
g_c	Conversion coefficient, in.-lbm/lbf sec 2
G	Mass velocity, lb/in. 2 sec
h	Heat transfer coefficient, Btu/in. 2 sec $^{\circ}$ R
k	Thermal conductivity, Btu/in.sec $^{\circ}$ R
K	Coefficient of Equation (1)
L	Heated length of tube, in.
Nu	Nusselt number, hD/k
P	Pressure, lbf/in. 2 (psia)
Pr	Prandtl number, $c_p \mu/k$
Q/A	Heat flux, Btu/in. 2 sec
r	Radius of curvature, in.
R	Tube radius, in.
Re	Reynolds number, DG/μ
T	Temperature, $^{\circ}$ R
V	Velocity, in./sec
St	Stanton number, $h/c_p V \rho$
ρ	Density, lbm/in. 3

μ	Viscosity, lbm/in.sec
ν	Kinematic viscosity, μ/ρ , in. ² sec
ϕ_1, ϕ_2	Factors in Equation (1)

Superscripts:

a, b, c, d	Exponents of dimensionless ratios in Equation (1)
------------	---

Subscripts:

b	Properties evaluated at the coolant bulk temperature, T_b
f	Properties evaluated at the film temperature, $T_f = 0.5 (T_b + T_w)$
He	Helix diameter, in.
ref	Reference temperature
w	Properties evaluated at the wall temperature, T_w

I. SUMMARY

This report compares experimental forced convection heat transfer data for cryogenic hydrogen with a number of equations that have been proposed for predicting liquid-side heat transfer coefficients for convectively-cooled rocket nozzles. Experimental data have been taken from tests in both straight and curved electrically-heated tubes at pressures ranging from 600 to 1500 psi and at coolant temperatures less than 200°R. The problem of extrapolating these equations to test conditions not explicitly achieved in experiments is also described.

Graphical comparison of the experimental data with empirical equations has demonstrated that for straight tubes at hydrogen temperatures below 200°R no equation correlates better than 76% of the data within limits of $\pm 20\%$ of that particular equation. A variable coefficient to account for deviations of the data at hydrogen temperatures below 100°R is recommended for each equation evaluated. The results of the analysis are two equations, one based on film temperature and the other on bulk temperature, which are believed to represent the test data for the straight tube tests. The curved tube test data are then compared with each of these equations.

II. INTRODUCTION

A severe heat transfer problem exists in the design of a regeneratively-cooled rocket nozzle with liquid hydrogen used as the coolant. Prediction of surface temperatures in the nozzle, particularly in the high heat flux throat region, often indicates that the coolant tubes will overheat and may possibly fail by thermal erosion. Where tolerable surface temperatures are predicted, the thermal gradients in the tube bundle can introduce severe stress problems. For the nuclear rocket nozzle, the designer is interested not only in knowing what wall temperatures will be experienced throughout the nozzle but also in how much energy will be removed by the coolant in terms of the increased enthalpy availability.

Integral to the above comments is the term "prediction". A workable nozzle design rests partly upon a proper characterization of the liquid-side (i.e., coolant side) heat transfer that will exist locally throughout the nozzle under the influence of the complex system-operating parameters. It follows that the more closely a prediction technique approaches the actual heat transfer condition, the more efficient the design. The purpose of considerable effort in this field is, thus, to achieve a workable prediction method which the designer can use with reasonable confidence.

Two basic approaches have been generally employed: (1) rigorous analyses based on boundary layer theory, and (2) empirical correlation of laboratory test data. Deissler (Ref. 1)* has developed an analytical technique to describe fully developed flow with variable fluid properties. Szetala (Ref. 2), however, could not correlate experimental hydrogen data using the Deissler approach. More recently, Hess and Kunz (Ref. 3) have attempted to evaluate selected experimental data of Szetala and of the Lewis Research Center, employing a similar analysis derived from the method of Wiederecht and Sonnemann (Ref. 4). Using a high-speed digital computer, approximately fifteen minutes were required to compute a single Nusselt number. Agreement with experimental data was good at low heat fluxes but

*A list of references is given on Page 54.

became progressively poorer as the heat flux was increased. It was concluded that the utility of the very complex method that finally evolved in this study was quite limited due to both the lengthy preparation and computer run times required for each point and to the fact that good agreement could only be achieved at high L/D values.

The second approach has been the development of closed-form correlations of the familiar form:

$$Nu = K Re^a Pr^b \phi_1^c \phi_2^d \dots \quad (1)$$

where K, a, b, c, d . . . represent constants derived empirically from single-tube test data and ϕ represents factors which allow for the non-ideal velocity and temperature profiles caused by extreme changes in fluid physical properties, passage geometry, etc. A conventional Nusselt-type equation, modified by a wall-to-bulk temperature ratio, has been employed widely in the past to correlate turbulent heat transfer data for cryogenic hydrogen at supercritical pressures. For example, the results of the initial heat transfer test program on cryogenic hydrogen conducted at Aerojet-General Corporation (Ref. 5) were predicted by an equation of the form

$$Nu_b = K Re_b^{0.8} Pr_b^{0.4} \left(\frac{T_w}{T_b} \right)^c \quad (2)$$

where K and c were experimentally-determined constants. Two equations were generated, depending in part upon the temperature difference between the wall and the coolant. At low wall temperatures (i.e., low fluxes and consequently low coolant temperatures), the unit heat flux was found to be proportional to a fractional power of the temperature driving force ($T_w - T_b$). At higher fluxes, for the same mass velocity, the unit heat flux was found to be proportional to the first power of the thermal driving force. This effect was believed to be associated more with the wall temperature achieved rather than the coolant temperature, mass velocity or heat flux level. Based on these data, two correlating equations, subsequently termed "A" and "B", were generated for predicting the test results.

"A" Equation:

$$Nu_b = 0.028 Re_b^{0.8} Pr_b^{0.4} (T_w/T_b)^{-0.64} \quad (3)$$

"B" Equation:

$$Nu_b = 0.0217 Re_b^{0.8} Pr_b^{0.4} (T_w/T_b)^{-0.34} \quad (4)$$

The experimental data from which these equations were generated were obtained in a series of tests with hydrogen flowing in a straight, uniformly-heated, 0.194-in. dia. tube with an 8.0-in. heated length. The tests were conducted with liquid hydrogen flowing at pressures of 680 to 1344 psia. The wall-to-bulk temperature ratios achieved in these tests ranged from 1.36 to 16.5.

At the inception of the NERVA program, the available heat transfer data for hydrogen at pressures above 400 psi and at temperatures both above and below the critical temperature were reviewed. Subsequently, an experimental heat transfer program was initiated to study the effects of geometry on the heat transfer to hydrogen at near-critical temperatures. In addition, considerable unpublished data* from tests on relatively long straight tubes were made available by R. C. Hendricks and R. W. Graham of NASA's Lewis Research Center. These data were analyzed, and attempts were made to correlate using various forms of the Nusselt equation.

* These data have since been published as Ref. 6.

III. EXPERIMENTAL TEST PROGRAMS

Various investigators have conducted experimental programs to determine the heat transfer characteristics of cryogenic hydrogen. In general, the majority of these experimental studies have been conducted using straight tubular test sections, resistance-heated by direct current. In these tests, the weight flow rate of the coolant is established and electrical energy applied to the test section. When the system achieves steady state, measurements are made of the power input, enthalpy change of the fluid, pressure level throughout the flow system, and outer wall temperatures along the heated length of the tube. From these measurements and a knowledge of the geometry of the system, the unit power generation in the tube, the local coolant temperature, and the temperature drop through the wall of the test section are determined. The local heat transfer coefficient is then computed for each of the various wall temperature thermocouple locations.

In all such tests of electrically-heated tubes, the local power generation is a function of the resistance of the metal tube. Thus, the local unit heat flux will vary depending on the local resistance of the tube and, where the coefficient of resistivity is temperature dependent, will depend on the temperature. In an electrically heated tube, the incremental voltage drop is constant when the temperature is uniform and the tube wall thickness and diameter are uniform, and hence the unit heat flux is uniform along the length of the tube. Likewise the weight flow rate or the mass velocity of the coolant for any steady state power level is constant, with the result that the computed local coolant temperature in such a test section increases linearly with heated length if specific heat is constant.

In application to nozzle design, it has been the practice to take data generated in such tests (i.e., constant diameter tubes flowing hydrogen at a constant mass velocity, at coolant temperatures between 40 and 100°R, and a constant unit heat flux at the wall) and to derive empirical equations to correlate it. These empirical correlations are then extrapolated to determine the heat transfer coefficients in a system in which the unit heat flux varies significantly both along the

length and around the "gas-wetted" portion of the flow channel periphery. Also, the flow channel does not have a constant diameter and hence the mass velocity is continually varying.

Lewis Research Center has measured the heat transfer coefficient to cryogenic hydrogen in long straight tubes. In these tests, the mass velocity was varied with a constant wall heat flux as the comparative parameter. At Aerojet, on the other hand, tests were performed using relatively short straight and curved tubes in which the mass velocity was held constant and the local heat flux varied. The primary difference in test results was the span of local coolant inlet temperature; for tests conducted at Aerojet, much higher heat fluxes were achieved, however, the span of coolant temperatures was less.

The test data obtained at Lewis Research Center in this early program informally transmitted to Aerojet in May of 1963, have now been published (Ref. 6). These data have been included in the correlating effort conducted at AGC and in the work reported by Hess and Kunz (Ref. 3) in which a predictive equation was proposed based on a film reference temperature correlation.

Experimental work conducted by Aerojet during this period (Ref. 7) included tests on the study of geometric effects in addition to straight tube tests, i.e., the effects of curvature on heat transfer and the associated non-uniform or asymmetric heat addition representative of a rocket nozzle coolant passage. More recently Hendricks et al. (Ref. 8) have completed and reported on a heat transfer program conducted at pressures ranging from 1000 up to 2500 psia. Some of the data in the latter report have been included in this study, specifically those data at pressures below 1500 psi.

IV. CORRELATION OF EXPERIMENTAL TEST DATA

Correlation of the experimental heat transfer test data has been attempted by comparing the experimental data with a form of Equation (1) with the physical properties evaluated at some reference temperature such as bulk, film or wall temperature. The ϕ term in Equation (1) has taken the form of a wall-to-bulk temperature ratio to some power, such as in Equations (2) and (3), or, as will be seen later, a term which is based on ratios of properties evaluated at the wall and bulk temperatures. The correlation of these experimental data has been attempted using two approaches: (1) a mathematical approach where the data were forced to fit a predetermined equation form by means of a regression correlation, and (2) a comparison of experimental data with empirical equations on a graphical basis to determine the equation which best represents the majority of the data. The range of certain test parameters for the experimental data included in this analysis are tabulated in Table I along with the total number of data points and the data source. For the design equations considered in the graphical analysis, the reference temperature, coefficients of the equation, and correction terms, if any, are tabulated in Table II.

A. COMPUTER REGRESSION ANALYSIS

The experimental heat transfer data obtained at Aerojet in tests of both straight and curved tubes with uniform heat addition were analyzed mathematically by means of a multiple regression analysis. An IBM 7094 computer program was prepared to handle five terms in determining the best exponents for the five variables and the coefficient of the equation. The multiple regression was performed on an equation of the form:

$$St = K Re^{a_1} Pr^{a_2} (1 + D/r_c)^{\frac{a_3 G^2}{\rho P g_c}} e^{a_4 (1 + D/L)} \left(\frac{T_w}{T_b} \right)^{a_5} \quad (5)$$

The bracketed term $(1 + D/r_c)$ was included in an attempt to allow for the tube curvature, and the term: $e^{a_4 (1 + D/L)}$ was included to allow for thermal entrance effects. The reference temperature could be selected as any ranging

TABLE I

RANGE OF TEST PARAMETERS

<u>Parameter</u>	<u>Maximum</u>	<u>Minimum</u>
Coolant-Side Wall Temperature, T_w , °R	1738	88
Wall-to-Bulk Temperature Ratio, T_w/T_b	20.8	1.8
Heat Flux Parameter, $\frac{(Q/A) D}{G^{0.8}}^{0.2}$, $\frac{\text{Btu}}{\text{lb}^{0.8} (\text{in. sec})^{0.2}}$	2.94	0.04
Diameter, D, in.	0.506	0.152
Length-to-Diameter Ratio, L/D	148	5.7

<u>Data Source</u>	<u>No. of Data Points</u>
Lewis Research Center (Ref. 6)	1054
REON Straight Tube (Ref. 7)	333
TN D-2977 (Ref. 8)	<u>438</u>
Total Points	1825

TABLE II

COOLANT-SIDE DESIGN EQUATIONS

Equation Form:	$Nu_{ref} = K Re_{ref}^{0.8} Pr_{ref}^{0.4} \phi_1^c \phi_2^d$	where $\phi_1 = T_w/T_b$			
Equation and Source	Reference Temperature	Equation Coefficient, K	Exponent c of ϕ_1	ϕ_2^d	Remarks
REON "A" (Ref. 5)	Bulk	0.028	-0.64	---	Recommended for low bulk temperatures
REON "B" (Ref. 5)	Bulk	0.0217	-0.34	---	
McCarthy-Wolf (Ref. 9)	Bulk	0.025	-0.55	---	
Dalle Donne-Bowditch (Ref. 10)	Bulk	0.024	$-(0.29 + 0.0056 L/D)$	---	
Hess-Kunz (Ref. 3)	$T_b + 0.5 (T_w - T_b)$	0.0208	---	$(1 + 0.01457 v_w/v_b)$	$Re_{ref} = \frac{DG}{\mu_f}$
Modified Film Correlation (Ref. 11)	$T_b + 0.5 (T_w - T_b)$	0.023	---	$(\rho_w/\rho_b)^{0.4}$	
Hendricks et al. (Ref. 8)	$T_b + 0.5 (T_w - T_b)$	0.021	---	---	Nusselt film correlation
Miller-Seader-Trebes (Ref. 12)	$T_b + 0.4 (T_w - T_b)$	0.0204	---	$(1 + 0.00983 v_w/v_b)$	

from the local bulk temperature to the local wall temperature. In addition to deriving the exponents a_1 through a_5 of the dimensionless parameters and the coefficient K of the equation, the standard errors associated with each exponent and the regression coefficient of the equation were obtained. By varying the reference temperature, it could be ascertained which reference temperature would permit the best fit. However, it was apparent from a review of the computer-derived error terms that the a_3 and the a_4 terms were not adequately characterizing the data; these factors were subsequently deleted from the analysis and the equation was reduced to the following three-variable form:

$$St_{ref} = K Re_{ref}^{a_1} Pr_{ref}^{a_2} (T_w/T_b)^{a_3} \quad (6)$$

where

$$T_{ref} = T_b + b_w (T_w - T_b)$$

The value of b_w could be varied from 1 to 0, resulting in a reference temperature T_{ref} ranging from the local wall temperature ($b_w = 1$) to the local bulk temperature ($b_w = 0$).

The computer-derived equation which best represented the test data obtained in straight tubes using the bulk temperature as the reference temperature was:

$$St_b = 0.017 Re_b^{-0.14} Pr_b^{0.96} (T_w/T_b)^{-0.8} \quad (7)$$

The regression coefficient for this equation was 0.689, indicating a relatively poor data fit. Subsequent attempts to improve the correlation using the term $e^{a_4 D/L}$ to characterize entrance effects or heated length effects were unsatisfactory. Reference (13) states that for a flow of water, the effect of sharp-edged entries can be accommodated by the term $1 + (D/L)^{0.7}$. Subsequently, this term was included in the analysis. Although this was effective in reducing the spread of data for L/D values of 18 or greater, it did not appreciably reduce the data spread at L/D values of 13 or less.

The equation which best represented the curved tube test data was

$$St_b = 0.0346 Re_b^{-0.17} Pr_b^{-0.3} (T_w/T_b)^{-0.7} \quad (8)$$

A reasonable data fit for this equation was indicated by a regression coefficient of 0.92.

One basic deterrent to the direct application of these mathematical expressions to design was the problem of extrapolating to conditions not covered by test data. Because of the somewhat poor data fit and strong dependence of the results on distribution of data it did not seem reasonable to apply these equations to design.

It was concluded that a regression analysis of data in the closed form Nusselt-type equation with the simple modifying factors employed does not adequately describe the complex heat transfer-fluid dynamic relationships existing in heating cryogenic hydrogen at high heat fluxes while flowing turbulently in even simple coolant passage geometries. Success with this approach must await a fuller understanding of turbulent heat transfer with a high degree of variability in fluid properties.

B. GRAPHICAL ANALYSIS

The forced convection heat transfer characteristics of liquids or gases at state conditions sufficiently removed from the critical region can be correlated by the familiar Dittus-Boelter equation without correction factors. In the case of oils, Sieder and Tate (Ref. 14), by introducing a viscosity correction factor, accounted for the large variation in properties between the hot film and the cold bulk fluid. However, it has not been demonstrated that experimental heat transfer data for fluids at state conditions near the critical region can be correlated by such an equation. For fluids in the region of their critical temperature and pressure, the thermodynamic and transport properties change non-uniformly with temperature and even pass through a point of inflection. It follows that the

shape of the characteristic velocity and temperature profiles across the diameter of the tube may bear little resemblance to the classical profiles for the fully-developed flow of a constant velocity fluid. Qualitative corroborative evidence may be found in the work of Wood (Ref. 15) with near-critical carbon dioxide, in which, for some tests, the maximum linear velocity was found to occur at y/r values from 0.1 to 0.4 (where y = distance from tube wall and r = tube radius) rather than at the center of the conduit ($y/r = 1$).

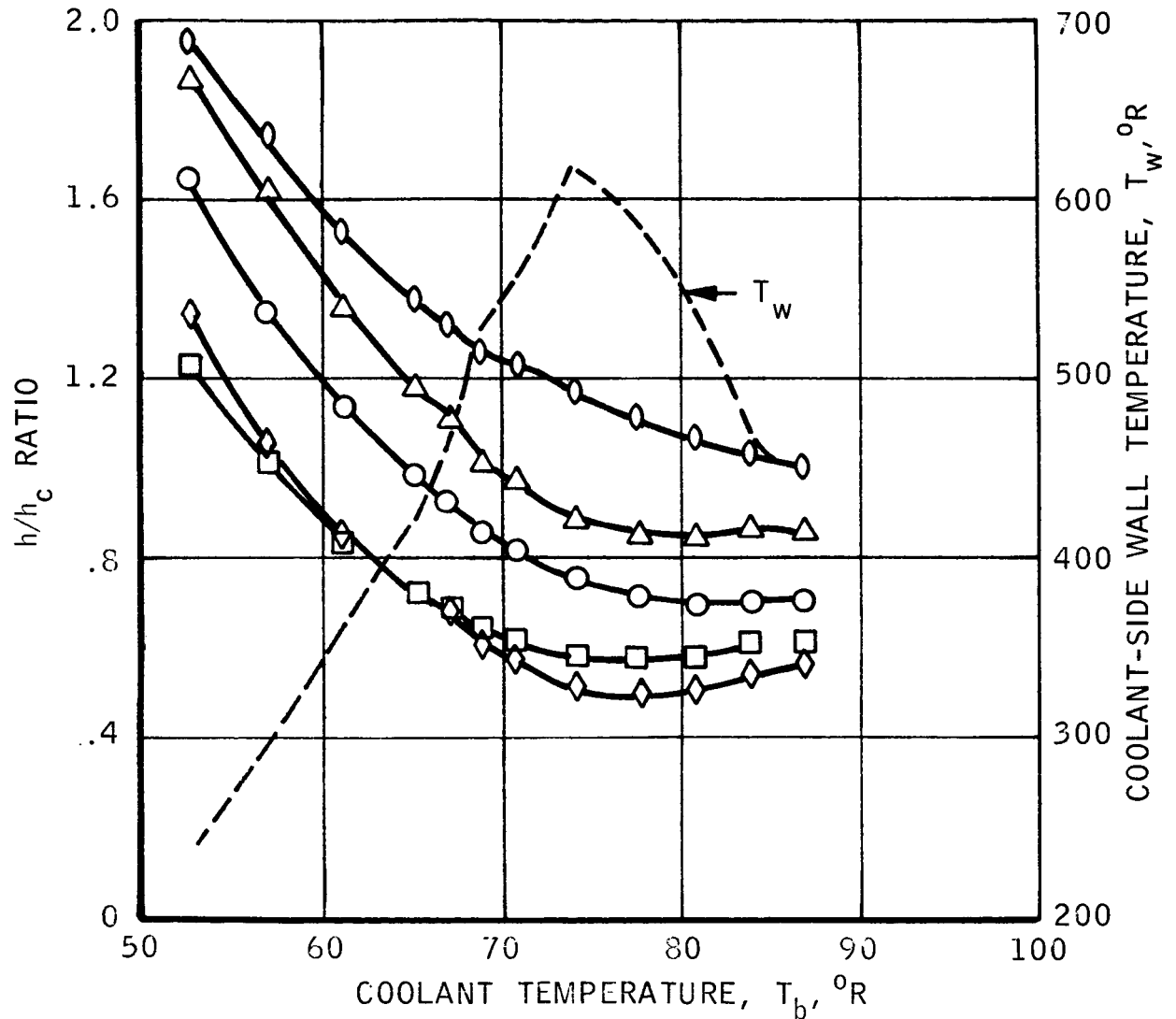
Lacking a well-defined physical model for heat transfer to hydrogen (particularly in the critical or transposed critical temperature region), it would appear that the conventional approach to correlation of the data will be satisfactory only if the correction factors applied to the equation (e.g., wall-to-coolant temperature ratio raised to some power) adequately allow for the differences in the shapes of the actual velocity and temperature profiles. Although a complete understanding of the physical model is not available, it has been assumed that the data can be represented grossly by the conventional equations. Certain experimental test data obtained from the Lewis Research Center (Ref. 6) have been compared with various correlating equations as illustrated by Figures 1 through 3. These data were selected as being representative of the manner in which the local wall temperature varies along a heated tube. For each of these tests, the experimental heat transfer coefficient, h , was divided by the heat transfer coefficient, h_c , calculated by specific design equations and the ratio plotted as a function of the coolant temperature. In addition, the coolant side wall temperature (computed from the measured outer-wall temperature and the power dissipated in the tube) has been plotted as a function of coolant temperature. Note that a ratio greater than 1.00 means the experimental h is greater than calculated, while a number less than 1.00 means the calculated h_c is larger than experimental. From these plots, it appears that the calculated ratios based on the suggested equations, although different, are nearly constant for the higher coolant temperatures or for that part of the tube where the wall temperature is decreasing with increasing length. For that portion of the tube where the wall temperature is increasing with increasing coolant temperature, the heat transfer coefficient cannot be adequately predicted by any of these equation forms.

SYMBOL AND EQUATION

DATA SOURCE

- REON "A" (REF. 5)
- ◇ REON "B" (REF. 5)
- MODIFIED FILM TEMP. (REF. 11)
- △ HESS & KUNZ (REF. 3)
- ◊ HENDRICKS, ET AL. (REF. 8)

REF. 6,
TEST 667



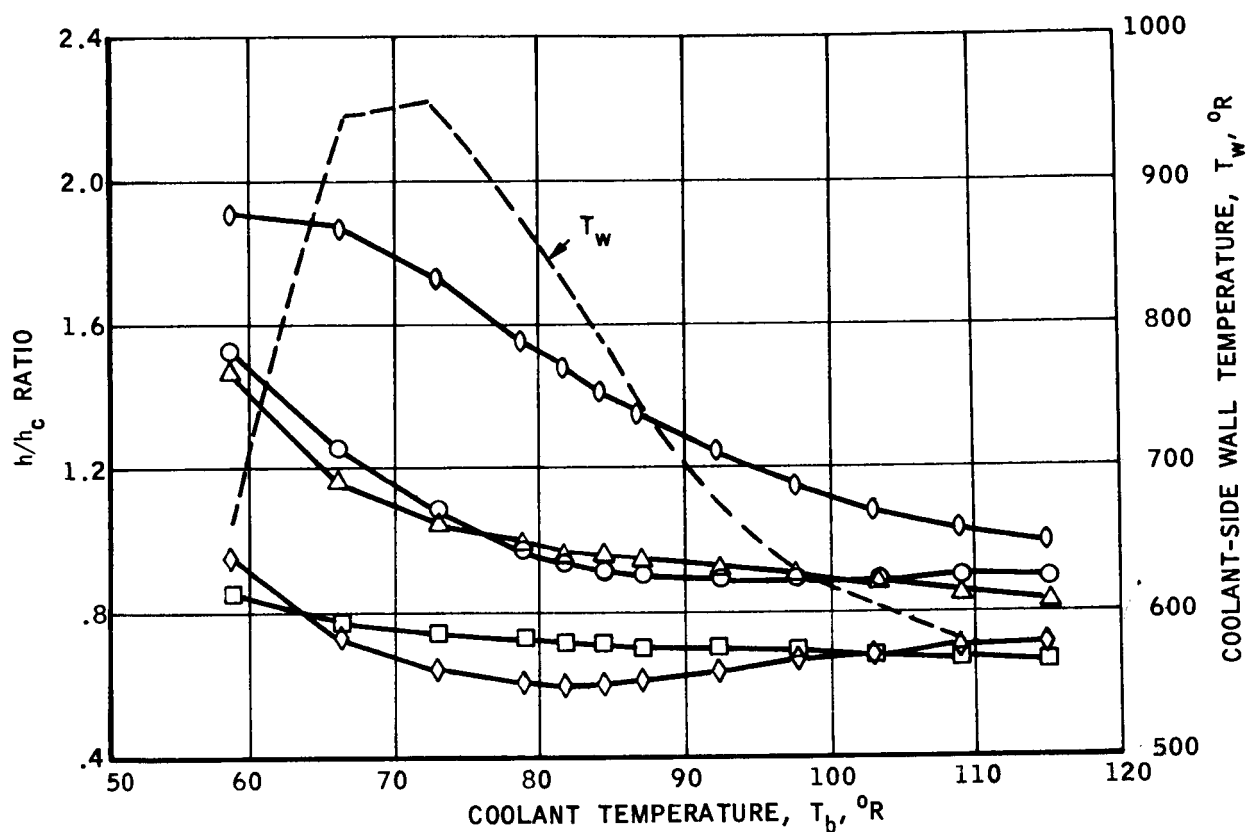
NOTE:

- h = EXPERIMENTAL HEAT TRANSFER COEFFICIENT
- h_c = CALCULATED HEAT TRANSFER COEFFICIENT

Figure 1

Comparison of Experimental and Predicted Heat Transfer Coefficients,
LRC Test 667 Data

<u>SYMBOL</u>	<u>EQUATION</u>	<u>DATA SOURCE</u>
○	REON "A" (REF. 5)	REF. 6,
◇	REON "B" (REF. 5)	TEST 708
□	MODIFIED FILM TEMP. (REF. 11)	
△	HESS & KUNZ (REF. 3)	
○	HENDRICKS, ET AL. (REF. 8)	



NOTE:

h - EXPERIMENTAL HEAT TRANSFER COEFFICIENT

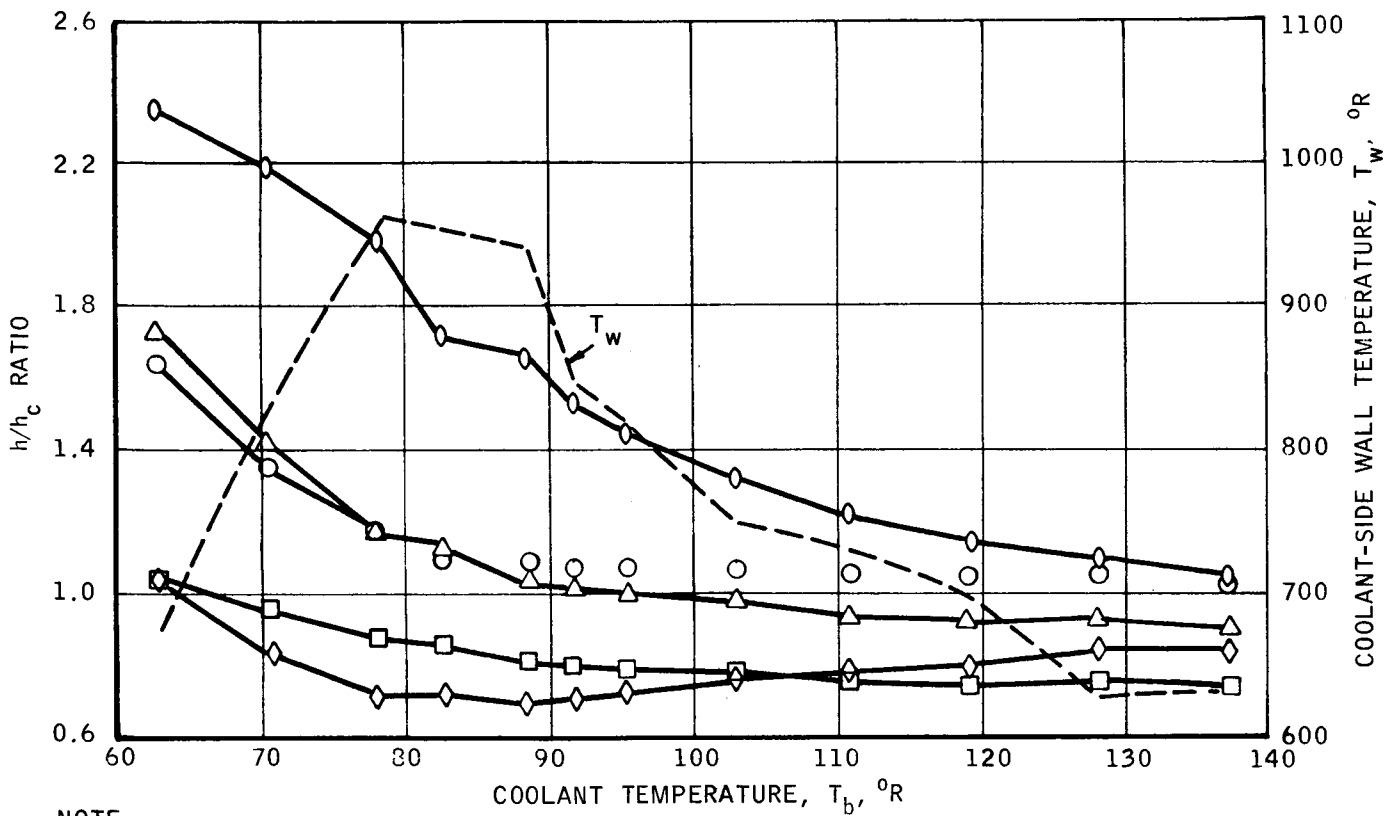
h_c = CALCULATED HEAT TRANSFER COEFFICIENT

Figure 2

Comparison of Experimental and Predicted Heat Transfer Coefficients,
LRC Test 708 Data

SYMBOL	EQUATION	DATA SOURCE
--------	----------	-------------

○	REON "A" (REF. 5)	(REF. 6)
◇	REON "B" (REF. 5)	TEST 881
□	MODIFIED FILM TEMP. (REF. 11)	
△	HESS & KUNZ (REF. 3)	
○	HENDRICKS, ET AL. (REF. 8)	



NOTE:

h = EXPERIMENTAL HEAT TRANSFER COEFFICIENT

h_c = CALCULATED HEAT TRANSFER COEFFICIENT

Figure 3

Comparison of Experimental and Predicted Heat Transfer Coefficients,
LRC Test 881 Data

By examining the way in which the heat transfer coefficient is predicted to vary in a tube with uniform heat flux and mass velocity for a span of coolant and wall temperatures, it is more apparent why the equations are relatively unsatisfactory at low coolant temperatures. Goldmann (Ref. 16) suggested that the dimensionless terms in any one of the equations can be separated into two groups. The terms which are a function of temperature and pressure are made equivalent to the balance of the terms which describe the geometry and heat flux characteristics of an experimental system. The result is a heat flux parameter, that has been referred to as the Goldmann parameter, which can be described as a function of temperature and pressure. The five equations used in the preparation of Figures 1 through 3 are again presented in Figures 4 through 8 in which the Goldmann parameter (lines of constant heat flux parameter, $(Q/A) D^{0.2}/G^{0.8}$) has been plotted as a function of the wall and bulk temperatures. These figures illustrate how the wall and coolant temperatures would be predicted to vary along a heated tube for constant values of the heat flux parameter, with data from three tests for comparison. It can be seen that the higher the heat flux parameter for any given coolant temperature, the higher the wall temperature predicted. Increasing coolant temperatures at any constant heat flux - mass velocity ratio, would result in reducing the wall temperature. Since the experimental tests have been conducted in systems where the heat flux parameter remains essentially constant throughout the length of the tube, the variation in coolant and wall temperatures should be predicted by a line of constant heat flux parameter.

The test data shown in Figures 1 through 3 were replotted in Figures 4 through 8 in terms of selected individual prediction equations. It is readily apparent that the wall temperatures as measured in the straight tube tests do not vary in the manner predicted by the design equations. In Figure 4 the variation in the relationship between the wall and coolant temperatures for lines of constant heat flux predicted by the REON "A" equation has been plotted. Figure 5 is the relationship predicted by the REON "B" equation, while Figure 6 shows the relationship predicted by a modified film temperature correlation. The other two relationships are for the Hess and Kunz equation (Figure 7) and the Nusselt film temperature equation (Figure 8).

SYMBOL	$\frac{(Q/A) D^{0.2}}{G^{0.8}}$	DATA SOURCE
		REF. 6
○	0.51-0.65	TEST 667
□	0.88-1.10	TEST 708
△	1.10-1.33	TEST 881

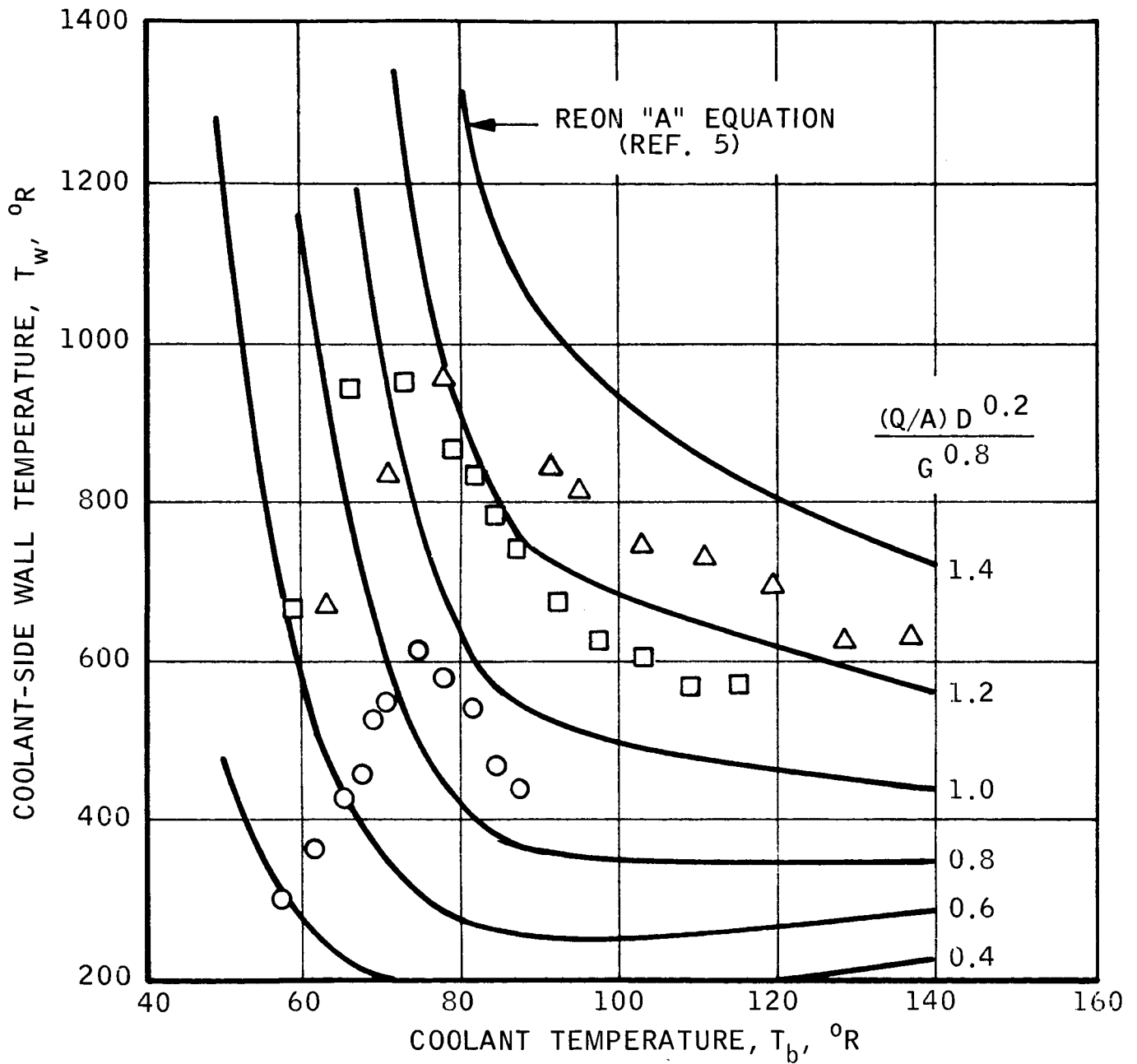


Figure 4

REON "A" Equation Predictions
in Terms of the Goldman Heat Flux Parameter
and Wall and Bulk Temperatures

SYMBOL	$\frac{(Q/A) D^{0.2}}{G^{0.8}}$	DATA SOURCE
		REF. 6
○	0.51-0.65	TEST 667
□	0.88-1.10	TEST 708
△	1.10-1.33	TEST 881

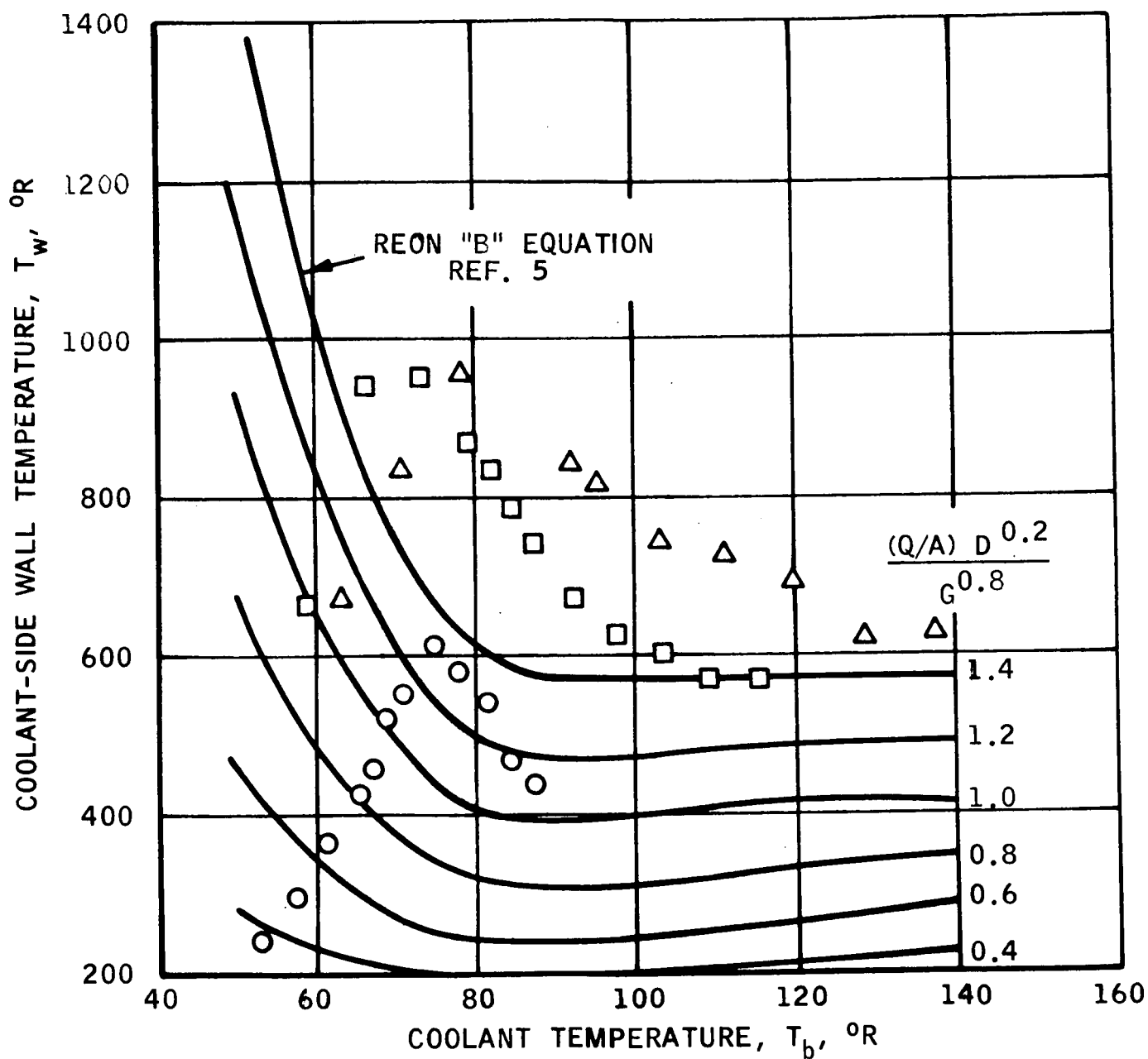


Figure 5

REON "B" Equation Predictions
in Terms of the Goldmann Heat Flux Parameter
and Wall and Bulk Temperatures

SYMBOL	$\frac{(Q/A) D^{0.2}}{G^{0.8}}$	DATA SOURCE REF. 6
○	0.51-0.65	TEST 667
□	0.88-1.10	TEST 708
△	1.10-1.33	TEST 881

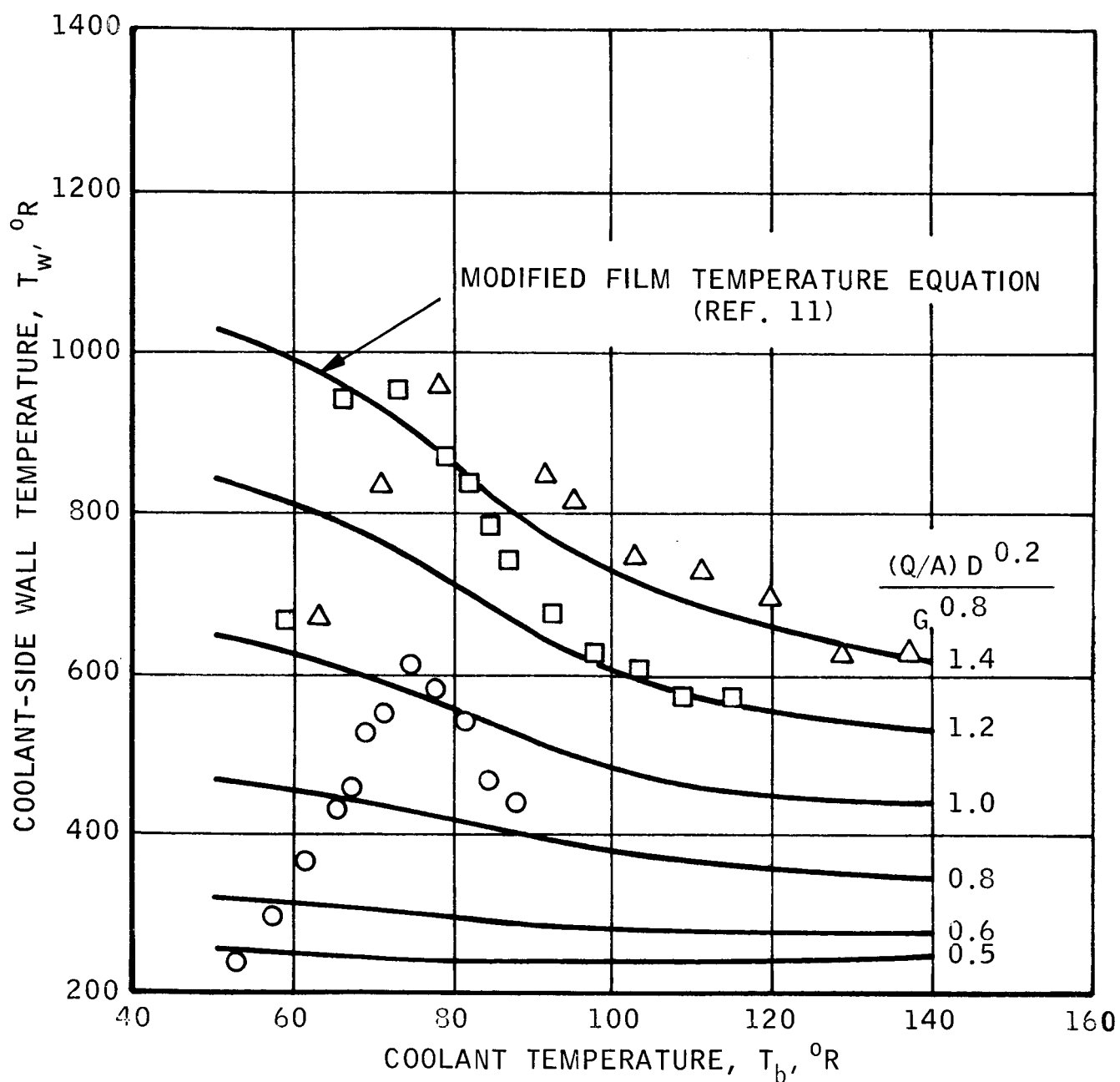


Figure 6

Modified Film Temperature Equation Predictions in Terms of
the Goldmann Parameter and Wall and Bulk Temperatures

SYMBOL $\frac{(Q/A) D^{0.2}}{G^{0.8}}$

DATA SOURCE
REF. 6

○	0.51-0.65	TEST 667
□	0.88-1.10	TEST 708
△	1.10-1.33	TEST 881

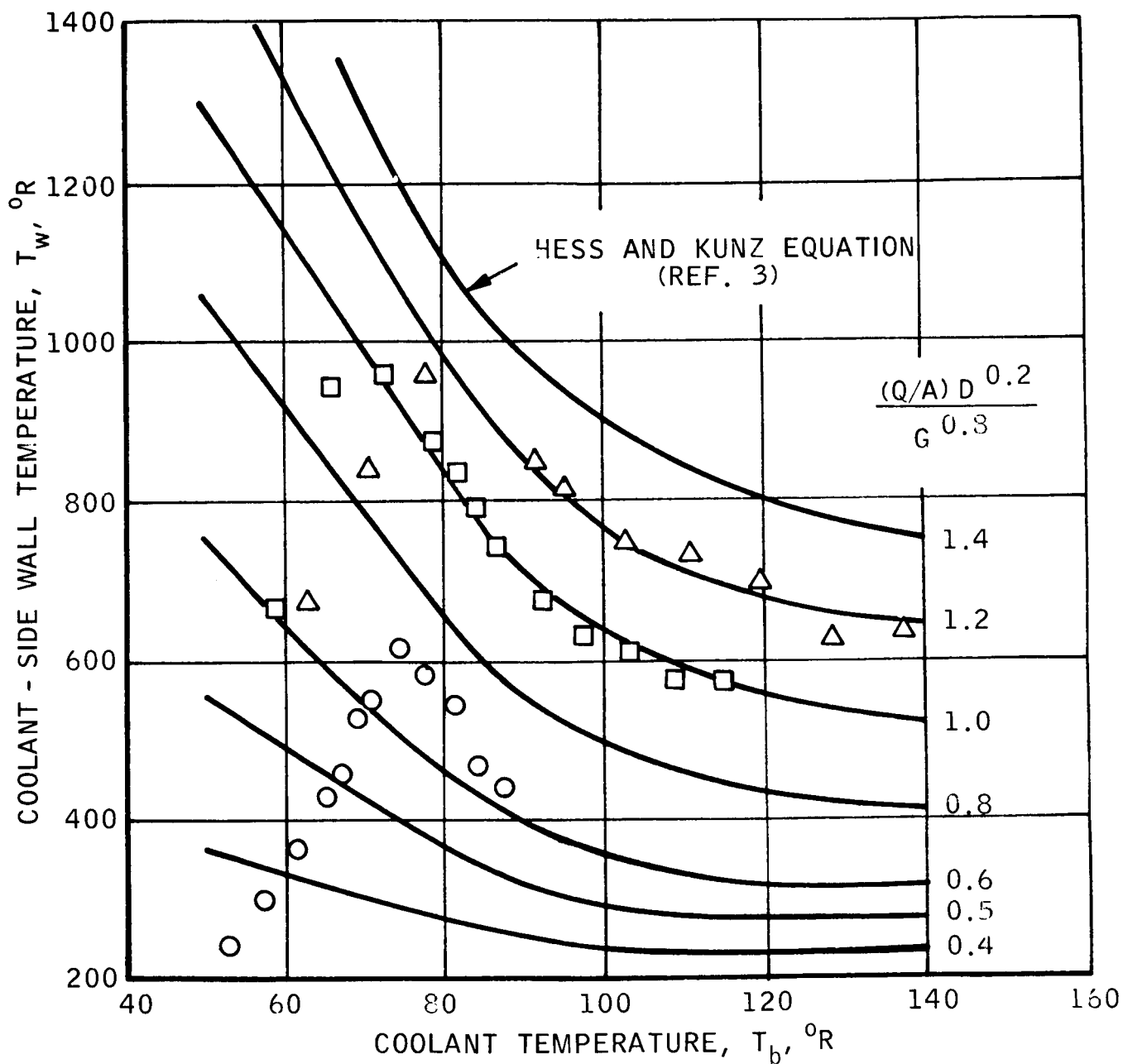


Figure 7

Hess and Kunz Equation Predictions in Terms of
the Goldmann Heat Flux Parameter and Wall and Bulk Temperatures

SYMBOL	$\frac{(Q/A)D^{0.2}}{G^{0.8}}$	DATA SOURCE REF. 6
○	0.51-0.65	TEST 667
□	0.88-1.10	TEST 708
△	1.10-1.33	TEST 881

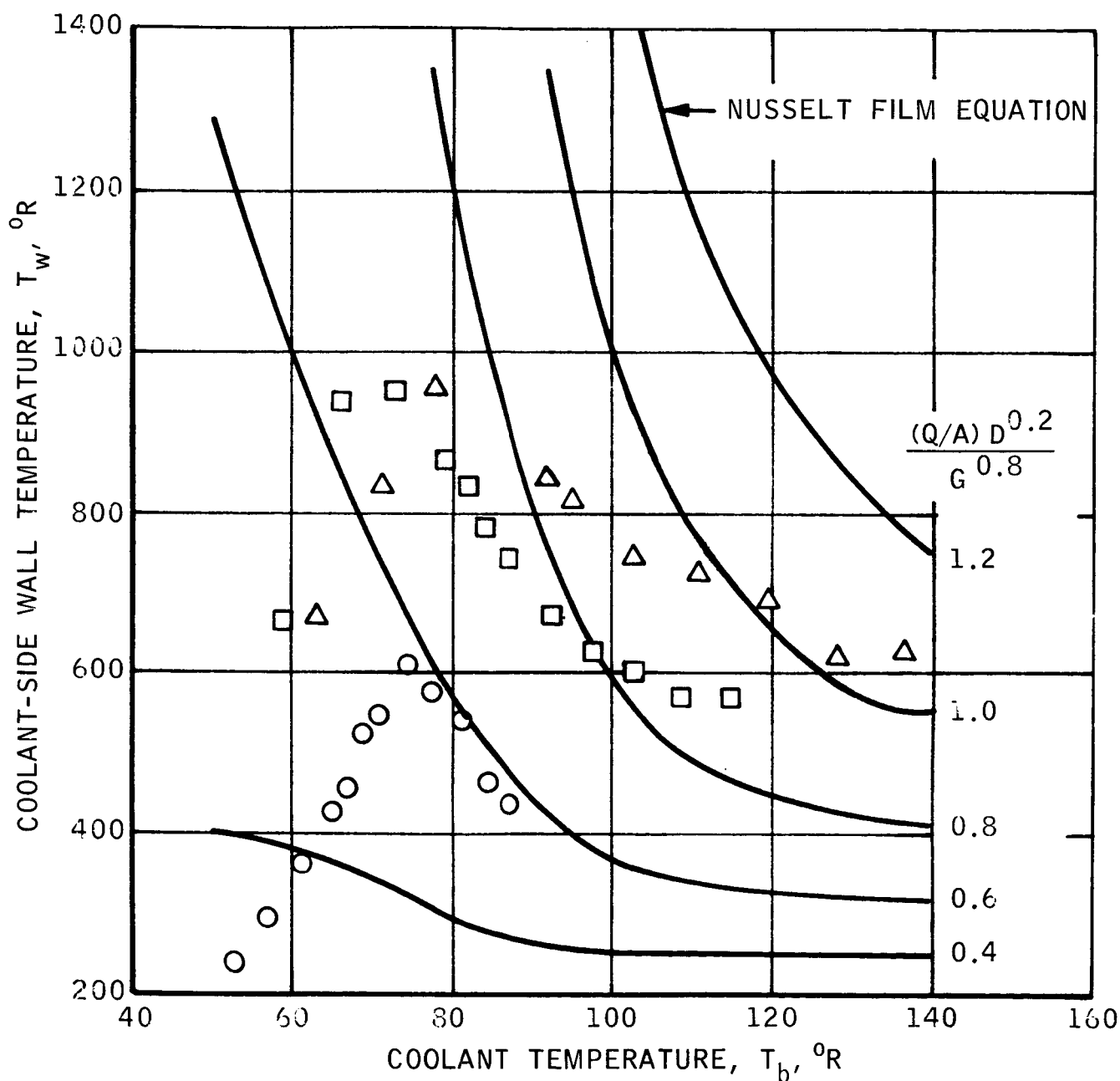


Figure 8

Nusselt Film Equation Predictions in Terms of
the Goldmann Heat Flux Parameter and Wall and Bulk Temperatures

Several observations can be made from these plots. In general, the predicted wall temperature at low coolant temperature increases rapidly with an increasing heat flux parameter. As the coolant temperature increases, the predicted wall temperature for the same heat flux parameter is predicted to decrease as the coolant temperature approaches 100°R and then is relatively constant at least to a temperature of 140°R. On each of these graphs, the data plotted on Figures 1 through 3 have been plotted and the range of the heat flux parameter for each of the three tests is noted. Data from Reference (6) were selected for this presentation because the characteristic change in wall temperature with coolant temperature is illustrated quite clearly. The data plotted are believed to be representative and are illustrative of the way the test data differ from the predicted. In general, the measured heat flux parameters are lower than predicted. On Figures 1 through 3, the high value of the h/h_c ratio at low coolant temperatures is representative of a low h_c because a high wall temperature is predicted by all the equations at low coolant temperatures.

A computer program was prepared to compute heat transfer coefficient ratios h/h_c where h_c is based on eight of the equations proposed for predicting the heat transfer coefficient for cryogenic hydrogen and to arrange the data for plotting. Prior to plotting, the data were sorted into three pressure levels; (1) less than 600 psi, (2) greater than 600 and less than 1000 psi, and (3) greater than 1000 psi.

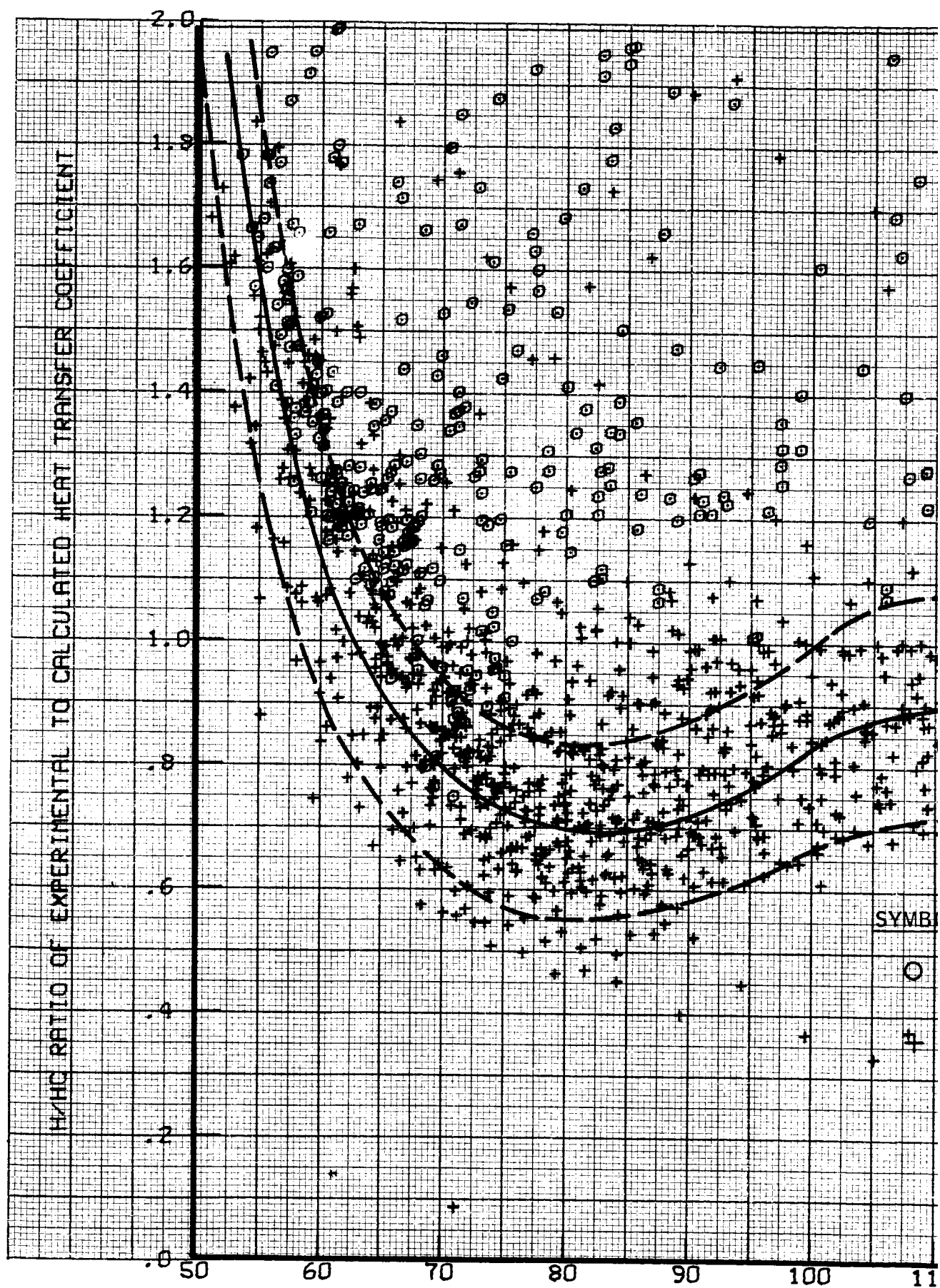
The physical properties used in the computation of the heat transfer coefficient were obtained from a tabular computer code for digital computers prepared at Los Alamos Scientific Laboratory and termed TAB-T. The properties in this code are for the temperature range from 36 to 5000°R and pressure from 0 to 1500 psi, hence the restriction to pressures less than 1500 psia.

C. BULK TEMPERATURE CORRELATIONS

Several equations based on the form of Equation (1) which use bulk properties have been recommended for the calculation of heat transfer coefficients. Four of these equations, as proposed in References 5, 9 and 10 for correlating hydrogen data, have been included in the analysis. The equations of Reference 5 were prepared specifically for liquid hydrogen and the equations of References 9 and 10 were prepared basically for gaseous hydrogen and helium.

The results of this analysis are given in Figures 9 through 12. These plots utilize experimental test data obtained in straight tubes from References 6 and 8. Several conclusions are evident from these figures. In general, all the equations result in a wide range in the magnitude of the h/h_c ratio. The predicted coefficient at low coolant temperatures is generally low, resulting in a ratio > 1 and, as the coolant temperature increases, the ratio generally decreases to a minimum at temperatures between 70 and 80°R. The ratio then increases to approach a value of unity as the coolant temperature increases. Significant scatter exists for the low temperature data; the high h/h_c ratio data are generally REON data while the Lewis Research Center data tend to be better correlated. The REON "B" and Dalle-Donne-Bowditch equations both tend to reduce the spread between the Lewis Research Center and the REON data better than do the REON "A" (Figure 9) or the McCarthy-Wolf (Figure 11) equations. The Dalle-Donne-Bowditch equation (Figure 12), however, shows a tendency to increase the spread in test data at bulk temperatures above 80°R into what appear to be two bands. The REON "B" equation (Figure 10) shows the least spread in the data of all the bulk temperature correlations; however, it also shows the greatest deviation from an h/h_c ratio of unity.

The differences in these four bulk temperature correlating equations are the exponents of the T_w/T_b ratio and the respective coefficients of the equations. The combined effect of these variations is shown by Figure 13. In that figure, the four bulk temperature equations have been plotted together to show that, as the T_w/T_b ratio increases, the Nusselt number (or heat transfer coefficient) decreases for the same Reynolds and Prandtl numbers. The low exponent of the REON "B" equation



REON "A" EQUATION

h = EXPERIMENTALLY-DETERMINED HEAT TRANSFER COEFFICIENT = $\frac{Q/A}{\Delta T_f}$

$$h_c = 0.028 \frac{k_b}{D} \left(\frac{D \rho_b v_b}{\mu_b} \right)^{0.8} \left(\frac{c_p \mu}{k} \right)_b^{0.4} \left(\frac{T_w}{T_b} \right)^{-0.64}$$

RECOMMENDED EQUATION TO NORMALIZE BULK TEMPERATURE EFFECTS USING $C_L = f(T_b)$

AS TABULATED

$$h_c = 0.028 C_L \frac{k_b}{D} \left(\frac{D \rho_b v_b}{\mu_b} \right)^{0.8} \left(\frac{c_p \mu}{k} \right)_b^{0.4} \left(\frac{T_w}{T_b} \right)^{-0.64}$$

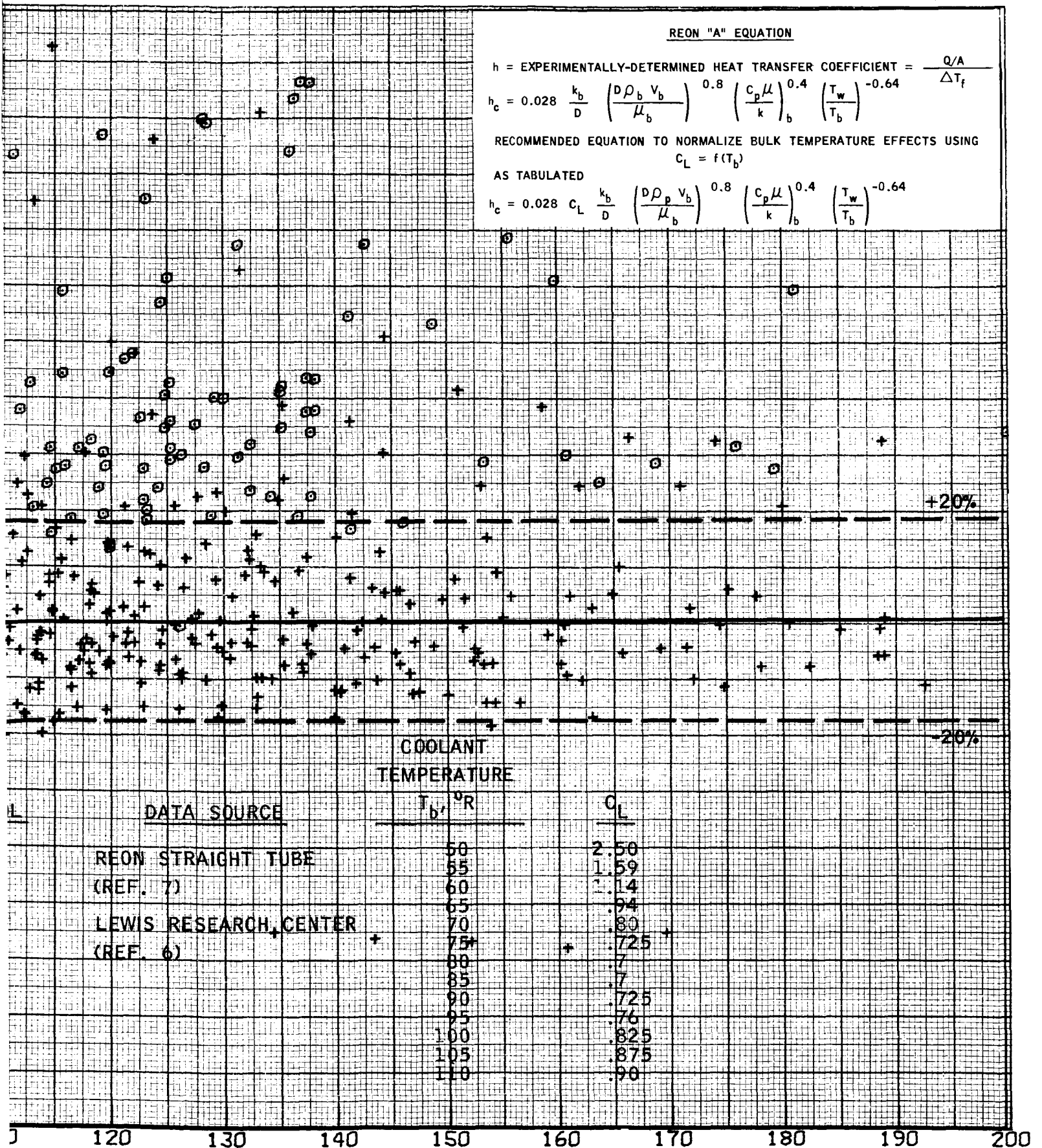
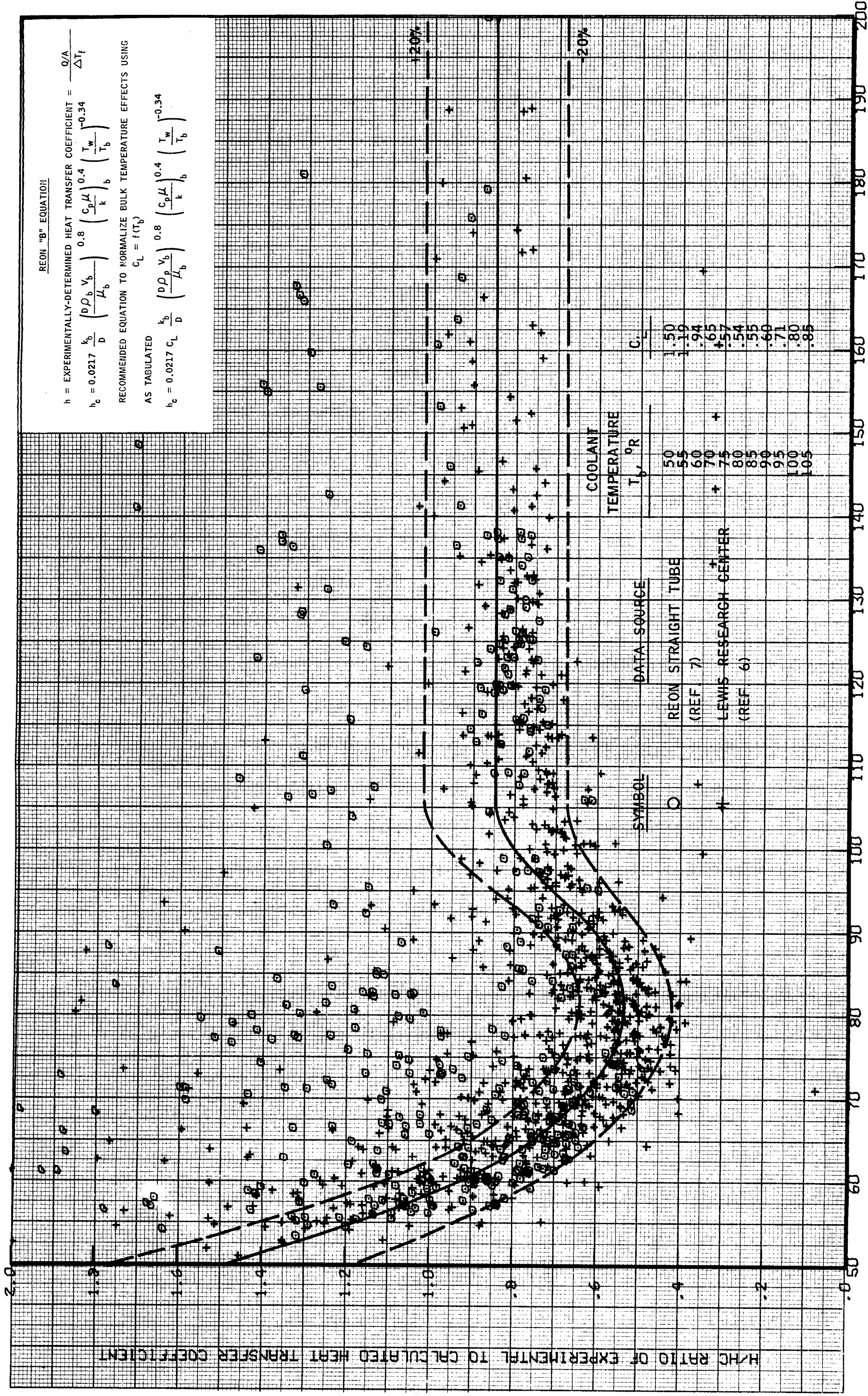


Figure 9

TEMP - DEG R

CON-3

Experimental/Calculated Heat Transfer Coefficient Ratio Comparison with the REON "A" Equation Prediction

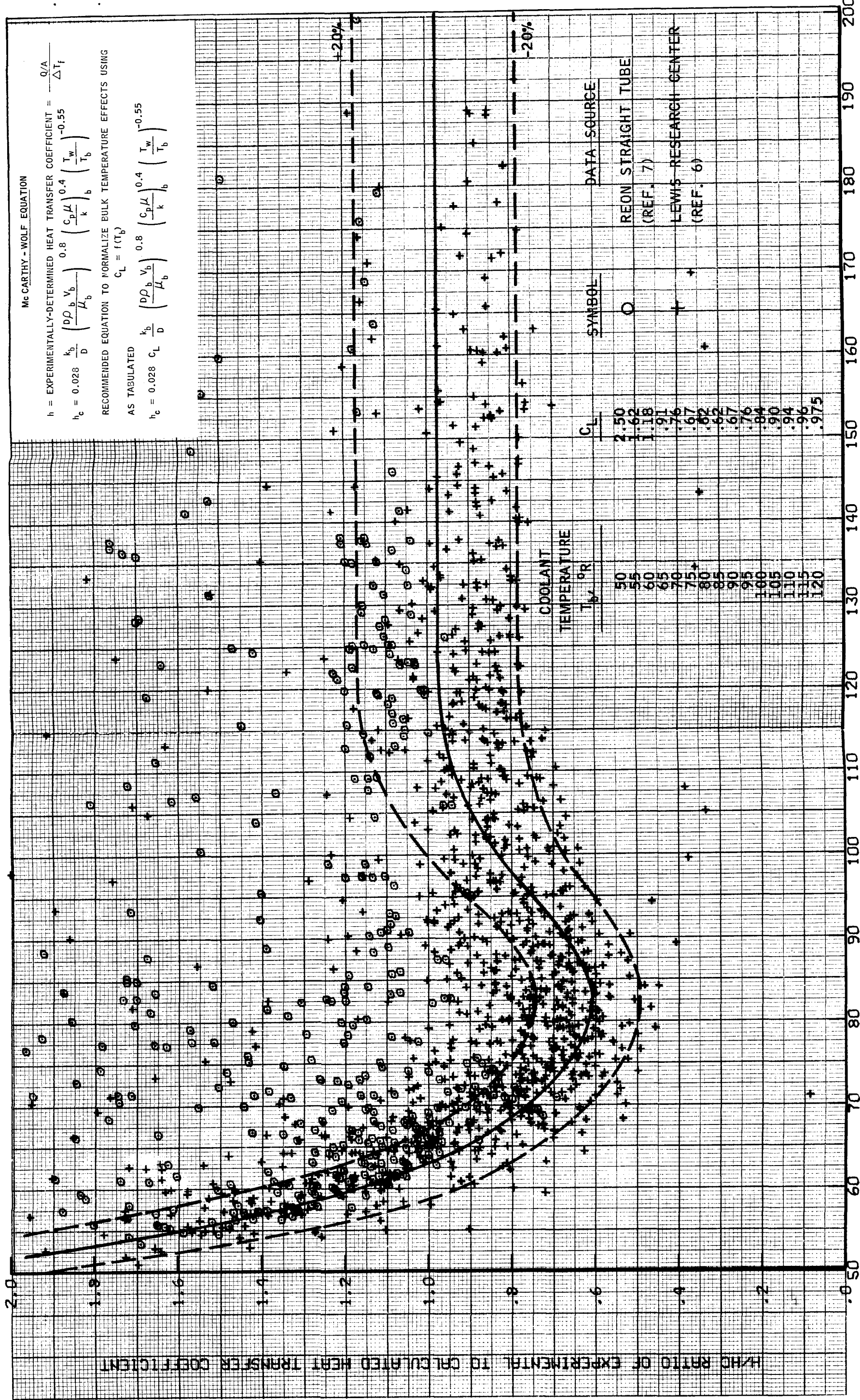


TEMP - DEG R

Figure 10

CON-2

Experimental/Calculated Heat Transfer Coefficient Ratio Comparison with the REON "B" Equation Prediction



Mc CARTHY - WOLF EQUATION

$$h = \text{EXPERIMENTALLY-DETERMINED HEAT TRANSFER COEFFICIENT} = \frac{Q/A}{\Delta T_f}$$

$$h_c = 0.028 \frac{k_b}{D} \left(\frac{D \rho_b V_b}{\mu_b} \right)^{0.8} \left(\frac{c_p \mu}{k} \right)_b^{0.4} \left(\frac{T_w}{T_b} \right)^{-0.55}$$

RECOMMENDED EQUATION TO NORMALIZE BULK TEMPERATURE EFFECTS USING

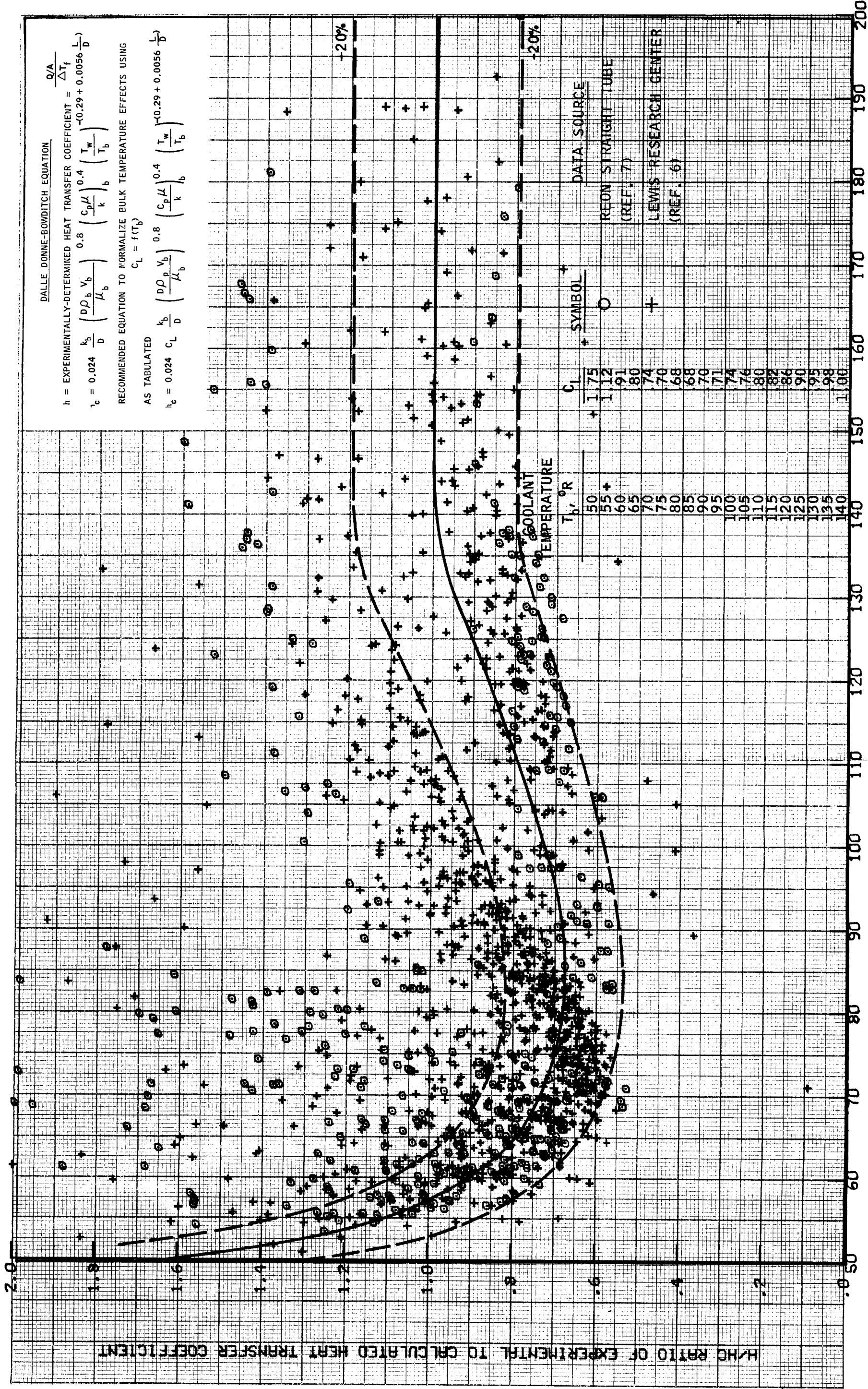
$$C_L = f(T_b)$$

AS TABULATED

$$h_c = 0.028 C_L \frac{k_b}{D} \left(\frac{D \rho_b V_b}{\mu_b} \right)^{0.8} \left(\frac{c_p \mu}{k} \right)_b^{0.4} \left(\frac{T_w}{T_b} \right)^{-0.55}$$

Figure 11 CON-4

Experimental/Calculated Heat Transfer Coefficient Ratio Comparison with the McCarthy-Wolf Equation Prediction



DALLE DONNE-BOWDITCH EQUATION

$h = \text{EXPERIMENTALLY-DETERMINED HEAT TRANSFER COEFFICIENT} = \frac{Q/A}{\Delta T_f}$

$h_c = 0.024 \frac{k_b}{D} \left(\frac{\rho \rho_b V_b}{\mu_b} \right)^{0.8} \left(\frac{c_p \mu}{k} \right)_b^{0.4} \left(\frac{T_w}{T_b} \right)^{-0.29 + 0.0056 \frac{L}{D}}$

RECOMMENDED EQUATION TO NORMALIZE BULK TEMPERATURE EFFECTS USING $C_L = f(T_b)$

AS TABULATED

$h_c = 0.024 C_L \frac{k_b}{D} \left(\frac{\rho \rho_b V_b}{\mu_b} \right)^{0.8} \left(\frac{c_p \mu}{k} \right)_b^{0.4} \left(\frac{T_w}{T_b} \right)^{-0.29 + 0.0056 \frac{L}{D}}$

Figure 12

CON-5

Experimental/Calculated Heat Transfer Coefficient Ratio Comparison with the Dalle Donne-Bowditch Equation Prediction

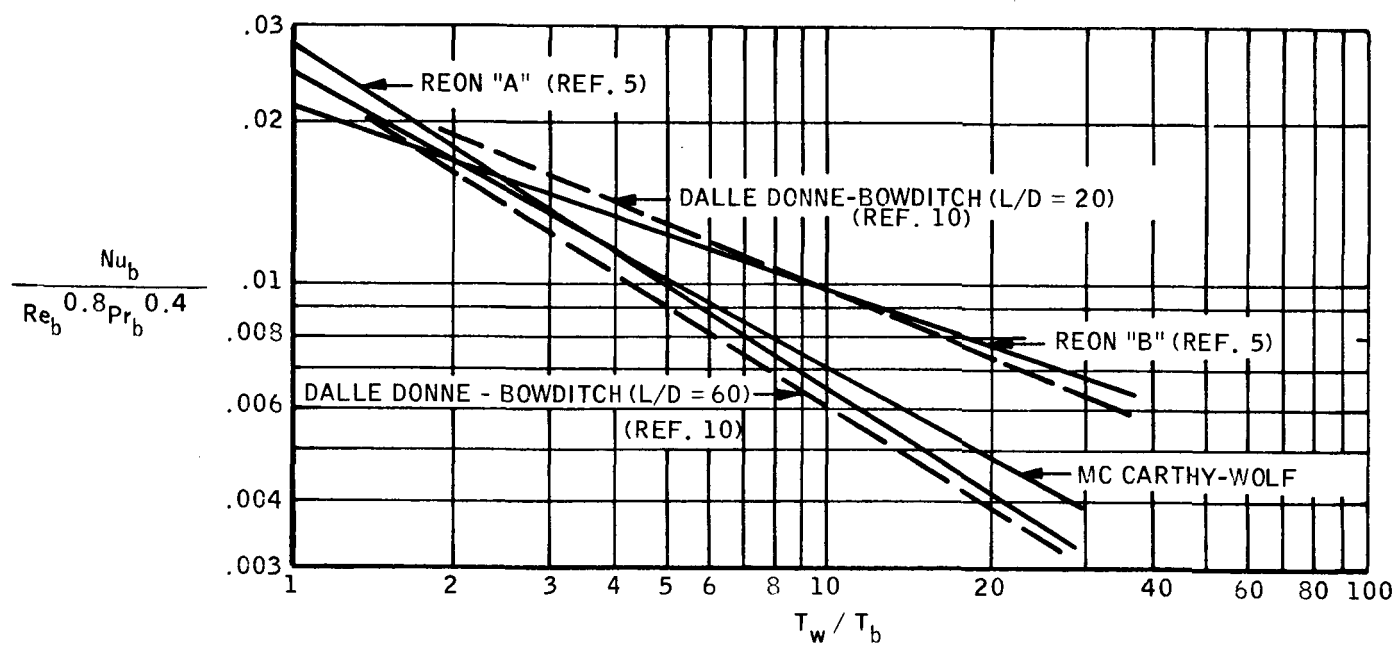


Figure 13

Comparison of Bulk Temperature Correlations for Liquid Hydrogen Heat Transfer

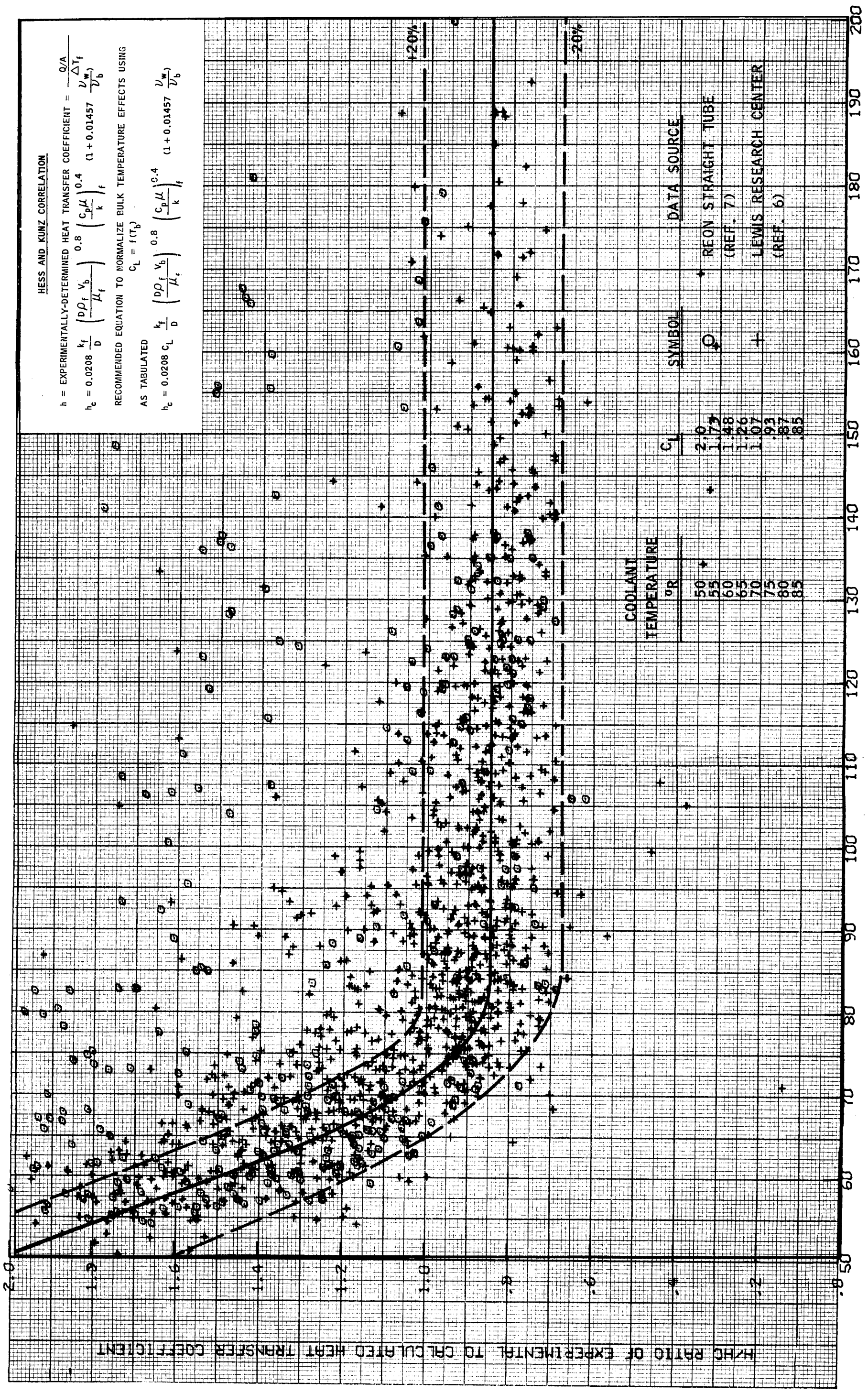
results in predicting a higher heat transfer coefficient than the REON "A" or the McCarthy-Wolf equations for T_w/T_b values greater than 3. In the case of the Dalle-Donne-Bowditch equation, a heated length-to-diameter ratio (L/D) of 20 results in a heat transfer coefficient similar to that predicted by the REON "B" equation while an L/D of 60 would result in the predicting of a heat transfer coefficient nearer that of the REON "A" or the McCarthy-Wolf equations. In general, high L/D values are associated with higher coolant temperatures, where the wall temperature is generally low and the ratio of wall-to-bulk temperature is small. However, for small L/D values the coolant temperature is generally low and the wall temperatures are often at a maximum, resulting in a fairly large T_w/T_b ratio and consequently a higher heat transfer coefficient is predicted. For example, at a coolant temperature of 80°R for a wall temperature of 800°R, the predicted heat transfer coefficient for an L/D of 20 would be 66% higher than if the L/D was 60, and all other conditions remained the same. A reduction in the coefficient of the T_w/T_b ratio from $-(0.29 + 0.0056 L/D)$ to $-(0.29 + 0.0019 L/D)$ is recommended by Miller and Taylor (Ref. 17). This would reduce the indicated spread in the predicted coefficient and would result in predicting a value between that predicted by REON "A" and REON "B" equations.

Williamson and Bartlit (Ref. 18) have reviewed the applicability of nine equations for predicting heat transfer to cryogenic hydrogen. These workers concluded that the data could be correlated by using the Dittus-Boelter equation with a coefficient of 0.0115. This equation can be compared with the other equations by drawing a horizontal line which intersects the "y" axis of Figure 13 at a value of 0.0115. It is readily apparent that the computed coefficients based on this equation would be lower than those predicted by the other equations at T_w/T_b values less than 3 and between the values predicted by the REON "A" and "B" equations for T_w/T_b values between 3 and 7 and greater than that predicted by the REON "B" for T_w/T_b values greater than 7. The modified REON "B" equation indicated on Figure 10 is believed to be the best correlating equation based on bulk properties. Although any of these bulk temperature equations (Figures 8 through 12) can be used for predicting the heat transfer coefficient by using the appropriate C_L value to adjust the coefficient of the equation, the REON "B" equation with variable C_L 's appears to minimize the apparent spread in test data and is suggested as best representing the data based on this analysis.

D. FILM TEMPERATURE CORRELATIONS

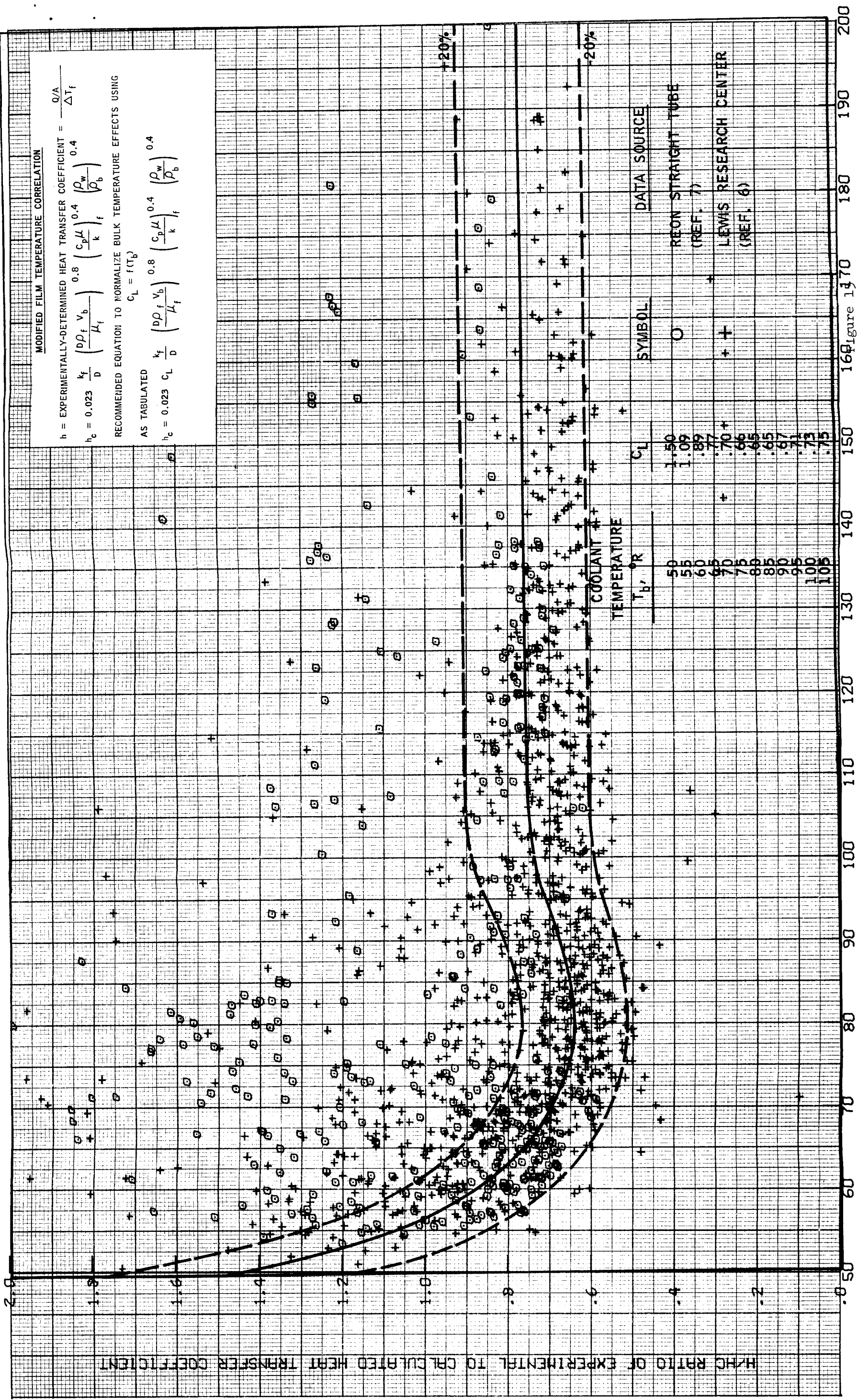
Correlation of the experimental data with physical properties evaluated at the film temperature would appear to be a valid approach since it can be reasoned that the hot layer of gas near the heated wall would tend to control the transfer of energy. Film temperature correlations, however, like bulk temperature correlations, still may require some correction term to account for the large variation in properties between the hot wall and the cold fluid core. Four equations based on film temperatures have been proposed for correlating hydrogen heat transfer data. Hess and Kunz (Ref. 3) proposed a film temperature correlation with a correction term involving a ratio of kinematic viscosities based on wall and bulk properties. At the Aerojet-General Corporation, a second equation (Ref. 17) was proposed and investigated by REON. This equation, termed the modified film temperature equation, incorporates a ratio of densities based on wall and bulk temperatures as a correction term. Hendricks et al. (Ref. 7) recently have correlated experimental test data at high pressures without a correction term by the Nusselt-film correlation. In addition, the Hess and Kunz film temperature correlation has been modified by Miller et al. (Ref. 18) for design purposes by modifying the constants in the original equation. Plots of these four equations are shown as Figures 14 through 17. The Hess and Kunz equation (Figure 14) shows the closest approach to unity at high coolant temperatures; the modified film temperature correlation (Figure 15), however, correlates the low temperature data better than any of the other equations. This is also suggested in Figure 6 where at low coolant temperatures the predicted wall temperature for lines of constant normalized heat flux do not increase almost asymptotically for decreasing temperatures, which is somewhat consistent with the experimentally determined wall temperature profiles. This was not true for each of the other equations.

The Nusselt film temperature correlation recommended by Hendricks (Ref. 8) (Figure 16) represents the Lewis Research Center data quite well, particularly at higher coolant temperatures. A comparison of the variation between REON and LRC data indicates that the Hendricks equation is conservative at the higher flux levels and high wall temperatures representative of the REON data. The equation



TEMP - DEG R

CON-0

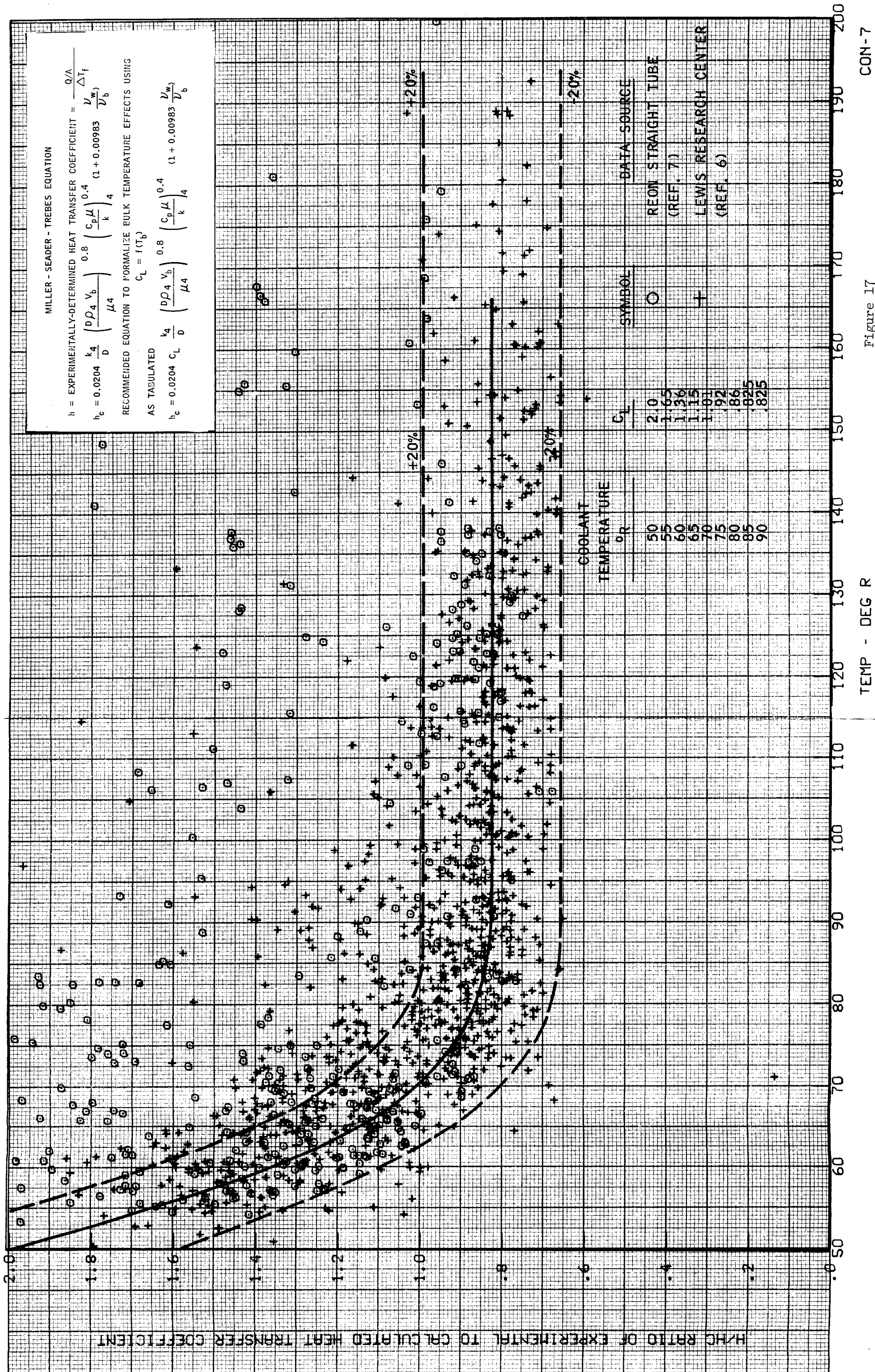


TEMP - DEG R Experimental/Calculated Heat Transfer Coefficient Ratio Comparison **CON-1**

the AGC Modified Film Temperature Equation Prediction

(Straight Tube Data)

34-2



CON-7

Figure 17

Experimental/Calculated Heat Transfer Coefficient Ratio Comparison with the Miller-Seader-Trebes Equation Prediction (Straight Tube Data)

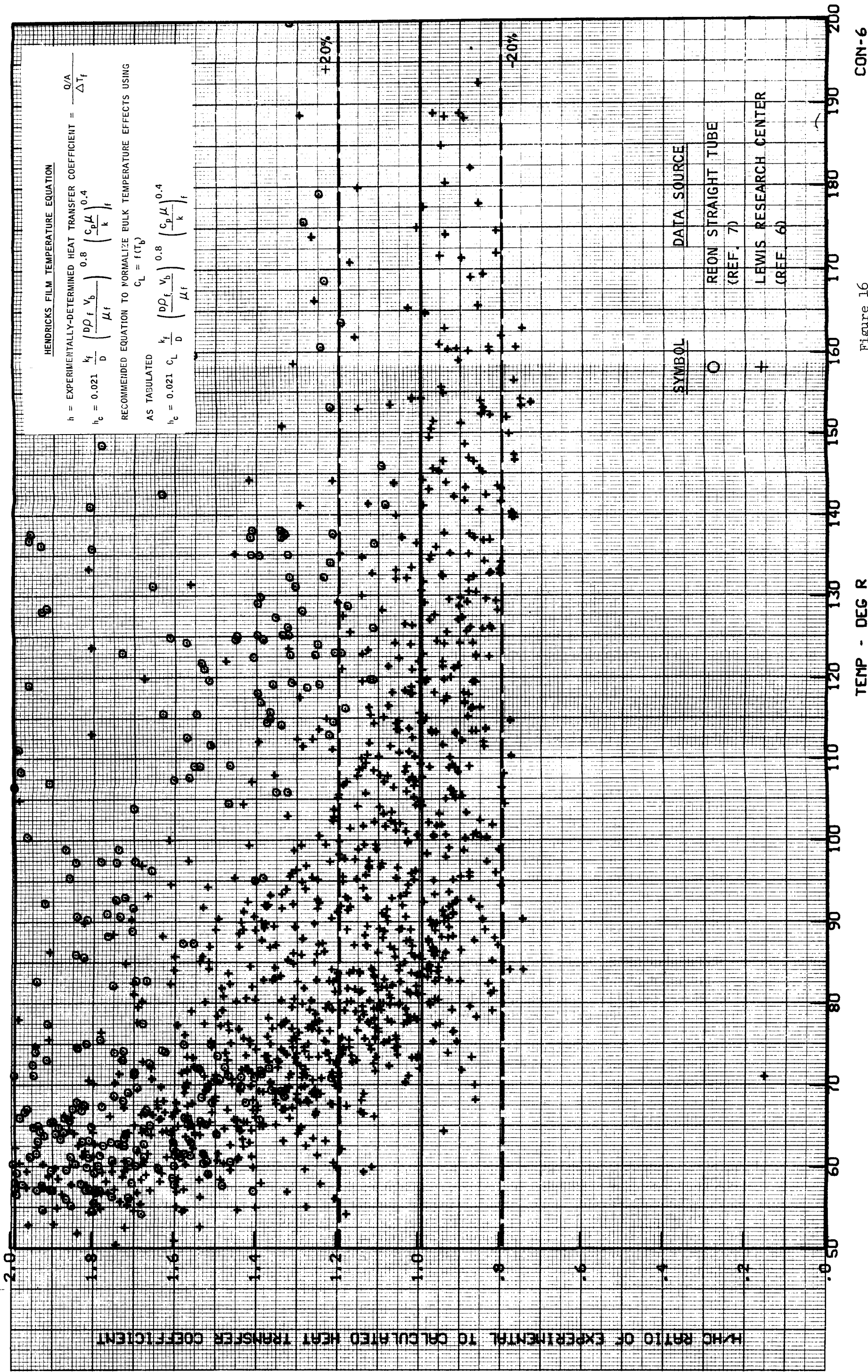


Figure 16

Experimental/Calculated Heat Transfer Coefficient Ratio Comparison with
the Nusselt Film Equation Predictions (Straight Tube Data)

proposed by Miller (Ref. 12) as a correlating equation for cryogenic hydrogen is shown in Figure 17 to be restrictive in the same manner as the other design equations. Actually, the difference between the Hess and Kunz and the Miller-Seader-Trebes equation is small, amounting to approximately 2.5% at coolant temperatures $> 85^{\circ}\text{R}$. As with the bulk temperature equations, the film temperature equations can be modified to represent the test data by factoring the coefficient of the equation by the appropriate C_L value. The Hess and Kunz equation modified by the appropriate C_L value adequately represents the test data compared in this analysis and is therefore recommended for use in design.

E. EFFECT OF SYSTEM GEOMETRY

The effects of coolant passage curvature on the heat transfer characteristics of cryogenic hydrogen have been investigated in tubes with symmetric and asymmetric heat addition. These tests were performed to determine the magnitude of any enhancement in the heat transfer coefficient due to the curvature and the application of this enhancement to design, specifically in the throat region of a nozzle.

Ito (Ref. 19) proposed that the effect of curvature on resistance to flow can be represented by the relationship:

$$\frac{f_{\text{curved tube}}}{f_{\text{straight tube}}} = \left[\text{Re}_b \left(\frac{R}{r} \right)^2 \right]^{0.05} \quad (9)$$

where:

Re_b = Reynolds number based on bulk properties

R = tube radius

r = radius of curvature

f = resistance coefficient

For the geometries characteristic of the test data depicted in Figures 18 and 19, and a Reynolds number of 10^6 , this relationship predicts an increase in resistance around the curve of approximately 30%.

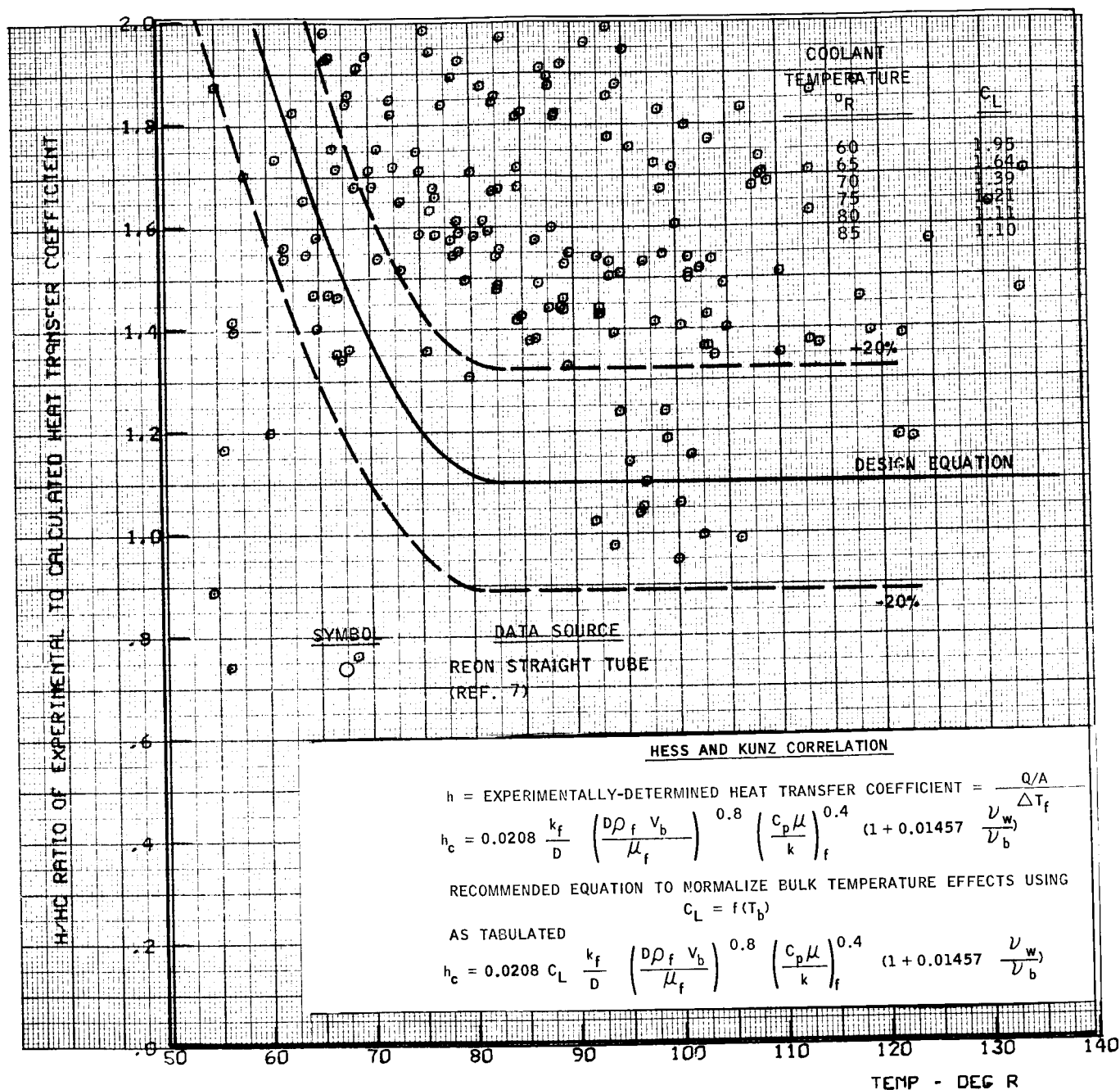


Figure 18

Experimental/Calculated Heat Transfer Coefficient Ratio Comparison with the Hess and Kunz Equation Prediction (Curved Tube Data)

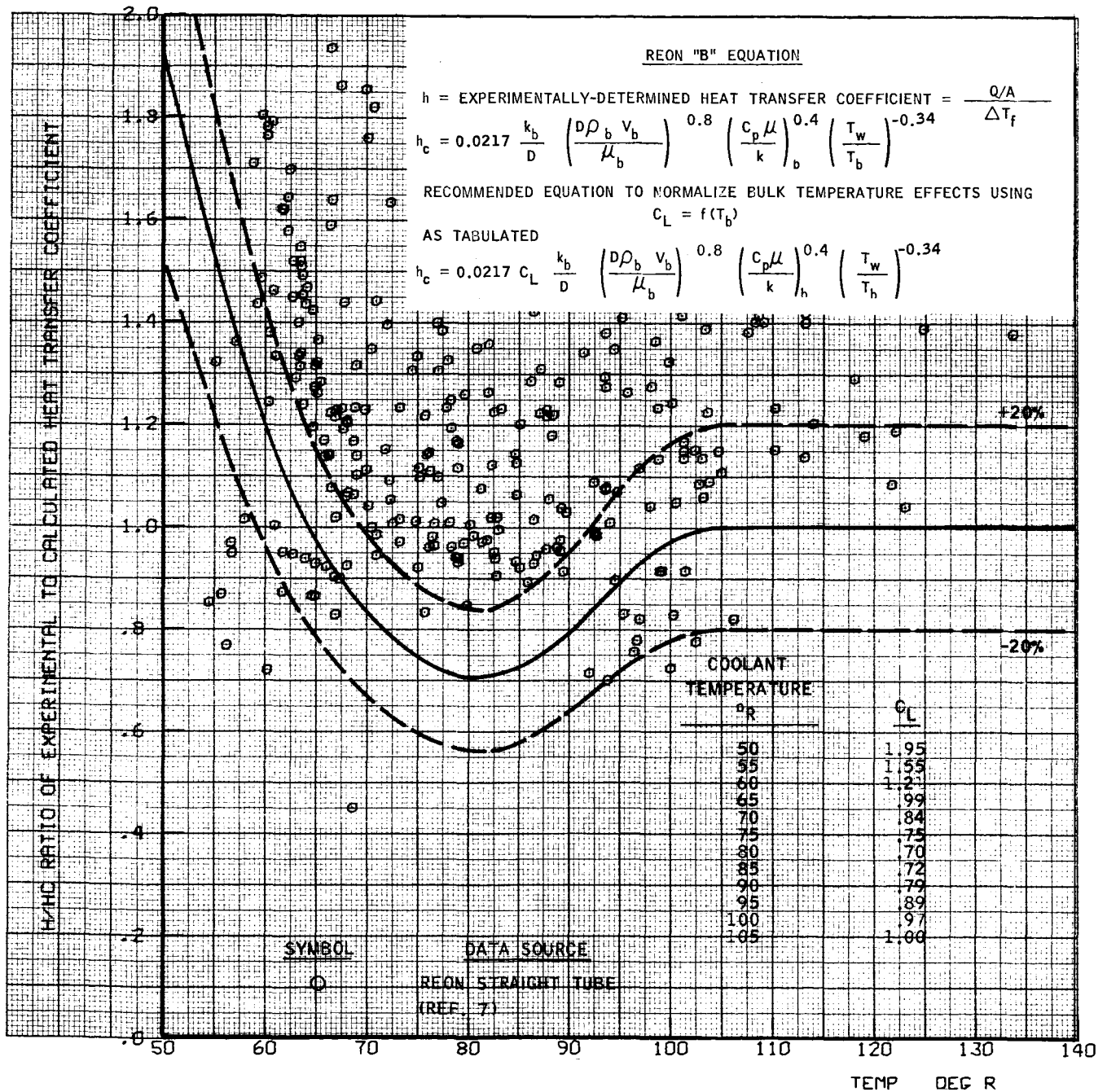


Figure 19

Experimental/Calculated Heat Transfer Coefficient Ratio Comparison with
the REON "B" Equation Prediction (Curved Tube Data)

For air flowing in coils, McAdams (Ref. 20) recommends the relationship of Jeschke where the average heat transfer coefficient for a coil exceeds that of a straight tube by a factor:

$$1 + 3.5 (D/D_{He})$$

where:

D = tube diameter

D_{He} = Helix diameter

Seban and McLaughlin (Ref. 21) found that, for the flow of water and oils in coils, the average heat transfer coefficient in coils with a D_{He}/D ratio of 17 was enhanced an average of 30% and at an D_{He}/D ratio of 104 was enhanced only 9%. These results correspond to enhancement per Jeschkes' prediction of 20 and 3%, respectively. The magnitude of the circumferential variation in local heat transfer coefficient was not characterized.

Hendricks and Simon (Ref. 22) studied the effect of curvature for sub-critical (two-phase), supercritical, and gaseous hydrogen flowing in four tube geometries. In general, they noted an enhancement of up to 3:1 between the concave (swept side of the tube) and convex (inside of the curve) sides with the coefficient on the convex side reduced but generally following the straight tube data at comparable conditions. The magnitude of the enhancement was found to be a function of the radius of curvature, angular position, and fluid conditions. A substantial difference in the heat transfer coefficient between the concave surface and the convex side was noted in these tests conducted in uniform wall thickness tubes. To better simulate nozzle conditions, tests performed at Aerojet were conducted using tubes with asymmetric heat addition at a flux ratio between the concave and convex sides of the tube of approximately 3:1. These tests also supported the finding that tube curvature results in enhancement. Consequently, the data obtained in tests in curved tubes have been considered separately in this analysis. The suggested design equations, both the film-temperature Hess and Kunz equation and the bulk-temperature REON "B" equation, were compared with the curved tube test data as shown on Figures 18 and 19. The conclusion drawn from these graphs is that for design purposes

a conservative value of the heat transfer coefficient for the curved portion of a nozzle would be predicted by the design line drawn as shown. In the case of the Hess and Kunz equation (Figure 18) at coolant temperatures above 80°R, a C_L value of 1.0 represents an enhancement of some 15 to 20% over the corresponding prediction for a straight tube. The enhancement factor to be used with the REON "B" equation is as indicated in Figure 19. This design line is equivalent to a 30% increase over the corresponding straight tube coefficient.

In the tests with asymmetric heat addition, the effect of angular position and radius of curvature were not determined. Some tests were conducted in uniform wall thickness tubes in which measurements were made at different angular positions and coolant temperatures to define the possible adverse curvature effect in the convergence-to-barrel section of the NERVA nozzle. In this region of the nozzle the curvature is such as to offer a possible reduction in heat transfer corresponding to the enhancement on the other side. The experimental data for the convex side of the tube has been compared with the Hess and Kunz equation prediction in Figure 20. It appears that the heat transfer coefficient is not significantly degraded from that in straight tubes and consequently this section can be handled analytically in the same manner as the straight tube portion of the nozzle.

DATA SOURCE (REF. 7)
TEST D95 LC-46

SYMBOL	L/D	LOCATION
○	9.6	STA. 1
□	16.7	STA. 2
◇	24	STA. 3
△	31	STA. 4

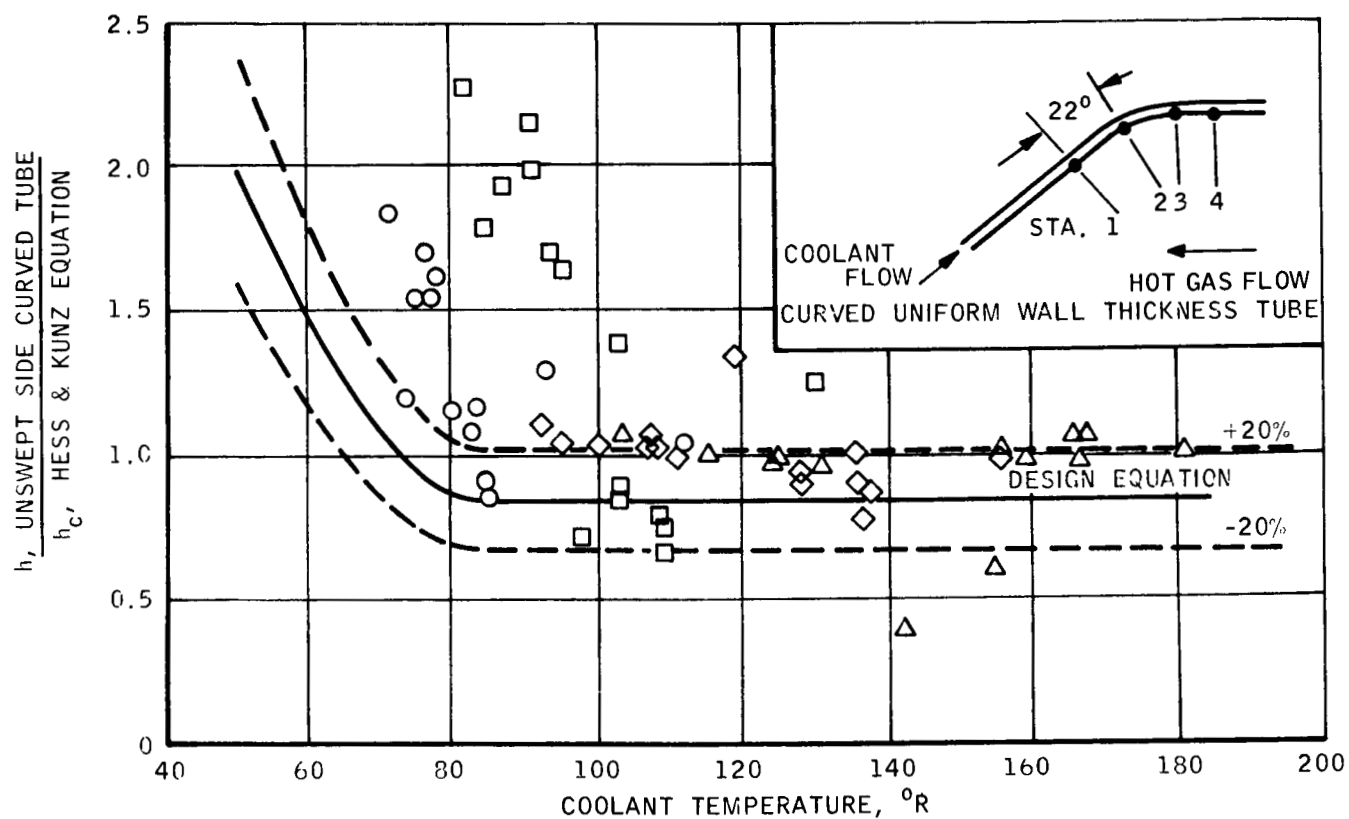


Figure 20

Comparison of the "Unswept" Side Heat Transfer Coefficient with
that Predicted by the Hess and Kunz Equation

V. DISCUSSION OF RESULTS

The results presented graphically in Figures 9 through 19 show that each equation predicts the data in essentially the same manner. In general, all equations result in considerable scatter both above and below the ideal value of $h/h_c = 1.0$. For design purposes, one is predisposed to select the most conservative heat transfer coefficient, and yet, for purposes of maximizing performance, the most conservative estimate is often not tolerable. It is therefore suggested that, as a conservative limit, the locus of the points along the lower edge of the family of points on any one of the figures be selected as representative of the minimum heat transfer case. By using this as a lower limit, a data band of $\pm 20\%$ and a nominal or design equation can be drawn. In this manner, the nominal design line and $\pm 20\%$ limit lines were established. Following the determination of these limits, the percentage of the data points encompassed by these limit lines was determined. In practice, this nominal equation is utilized in design by defining a coefficient multiplier of the equation as the value of the ordinate at any temperature, i.e., a liquid-side coefficient, or " C_L ", which is a function of the coolant temperature. The C_L values for each equation included in this report are listed on the respective graphs. It is apparent that any one of the equations then can be applied to design by proper selection of the C_L values, and the primary difference between the equations becomes the confidence level based on the percentage of points located within the design limits.

From this analysis, it has been demonstrated that two equations reasonably describe the test data when factored with a C_L multiplier: (1) for a film temperature correlation, the Hess and Kunz equation, as represented on Figure 14 in association with the proper C_L versus coolant temperature relationship, adequately represents the data; and (2) for the case of a bulk temperature correlation, the REON "B" equation properly corrected by the C_L versus coolant temperature relationship, as represented in Figure 10, presents the most representative bulk temperature correlation.

The percentage of experimental points falling within $\pm 20\%$ of the design equation on each of the graphs is tabulated on Table III.

The design of a regeneratively or convectively cooled nozzle using liquid hydrogen as a coolant is performed on a digital computer, hence the complexity of the correlating equations is not a formidable problem. The nozzle design computer program in use at Aerojet "guesses" bulk temperature, gas-side temperature, coolant-side temperature and pressure, and iterates on these four parameters until the system is consistent. The computations are performed in a stepwise manner at specific points along the coolant channel using the values from the previous station as guesses for the following channel increment.

These stepwise calculations are necessary in order to determine the coolant temperature rise due to enthalpy change and the total pressure drop in the nozzle along the coolant passage. Since the coolant flow area is not constant but decreases as the throat region is approached, the maximum pressure drop occurs in the region of the throat and, consequently, a small variation in the computation of the local coolant temperature can result in an appreciable variation in the magnitude of the total pressure drop calculated. One check on the adequacy of any set of gas- and liquid-side heat transfer correlations has been based on how well the computed overall pressure drop and overall coolant temperature rise, as predicted by analysis, match the measured parameters from nozzle tests.

At the present time a factored form of the Hess and Kunz film temperature equation is used by the NERVA nozzle design group in the design of the convective-cooled U-tube nozzle. For the straight section of the nozzle, 85% of the calculated coefficient is used in design, while 100% of the coefficient is used in the nozzle throat region between the points of tangency. Based on the analysis presented herein, the coefficient of the equation would be a variable function of the coolant temperature, in effect changing the method of calculating the coefficient only in the divergent portion of the nozzle. This is illustrated by Figures 21 through 23. These plots are based on test data from reactor tests of the NERVA nozzle S/N-022. In each case the calculated parameter has been plotted

TABLE III

PERCENTAGE OF POINTS FOR h/h_c RATIO WITHIN + 20% OF THE
 C_L DESIGN LINE ON FIGURES 9-12 AND 14-17

<u>Reference Equation</u>	<u>Percentage</u>	<u>Figure</u>
REON "A" (Ref. 5)	71	9
REON "B" (Ref. 5)	76	10
McCarthy-Wolf (Ref. 9)	66	11
Dalle-Donne-Bowditch (Ref. 10)	66	12
Hess-Kunz (Ref. 3)	78	14
Modified Film Temperature (Ref. 11)	69	15
Nusselt Film Temperature (Ref. 8)	--	16
Miller-Seader-Trebes (Ref. 12)	76	17

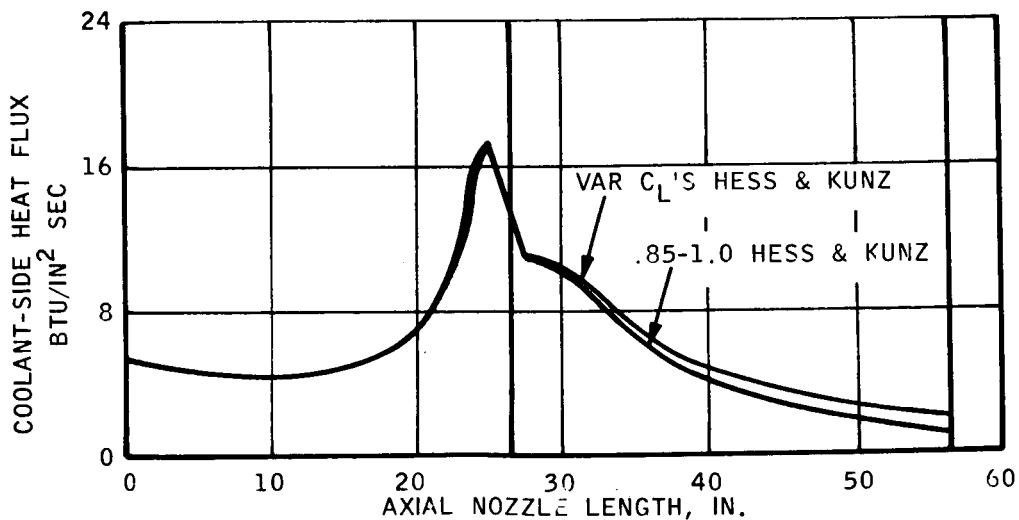
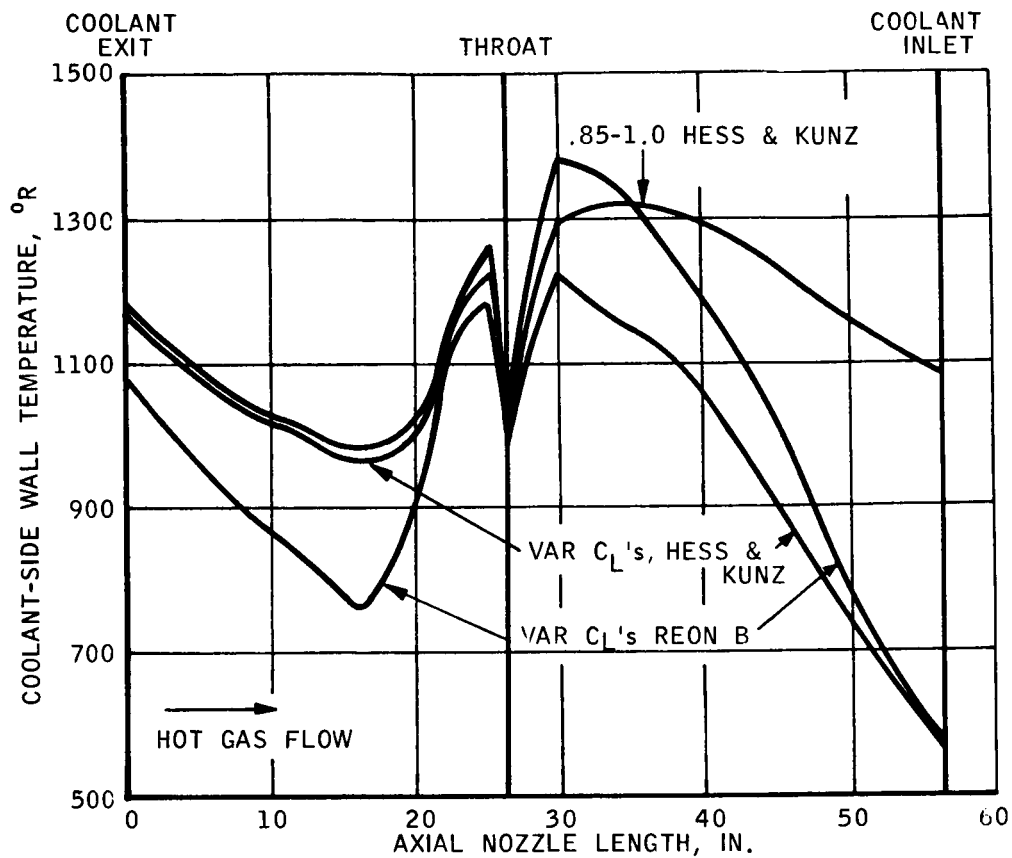


Figure 21

Coolant-Side Wall Temperature and Heat Flux Profiles for
S/N-022 NERVA Nozzle as Predicted by the Nominal Hess and Kunz Design Equation
and the Hess-Kunz and the REON "B" Equations with Variable C_L Values

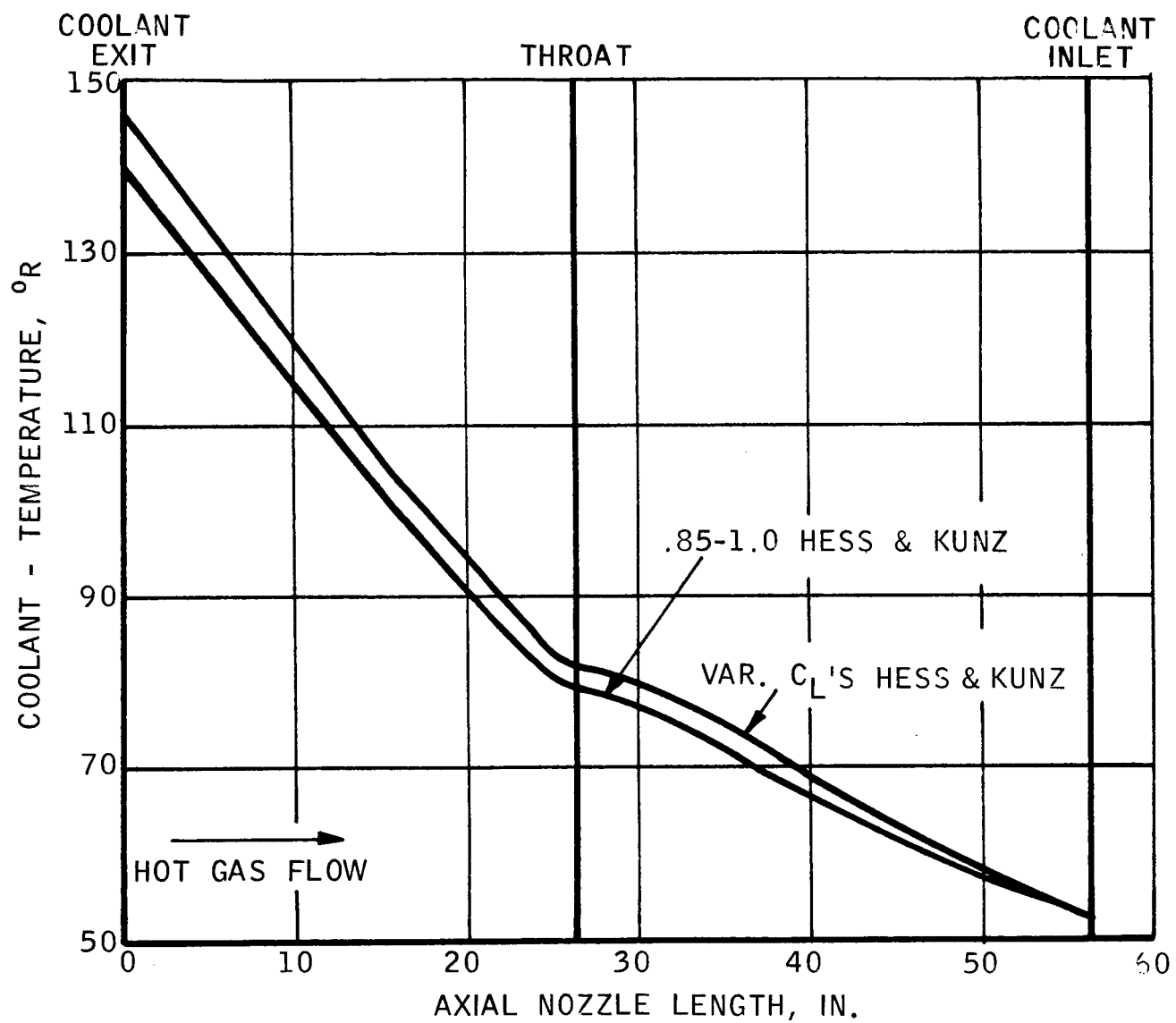


Figure 22

Coolant Bulk Temperature Profile for
S/N-022 NERVA Nozzle as Predicted by the Nominal Hess and Kunz Design Equation
and the Hess and Kunz Equation with a Variable C_L

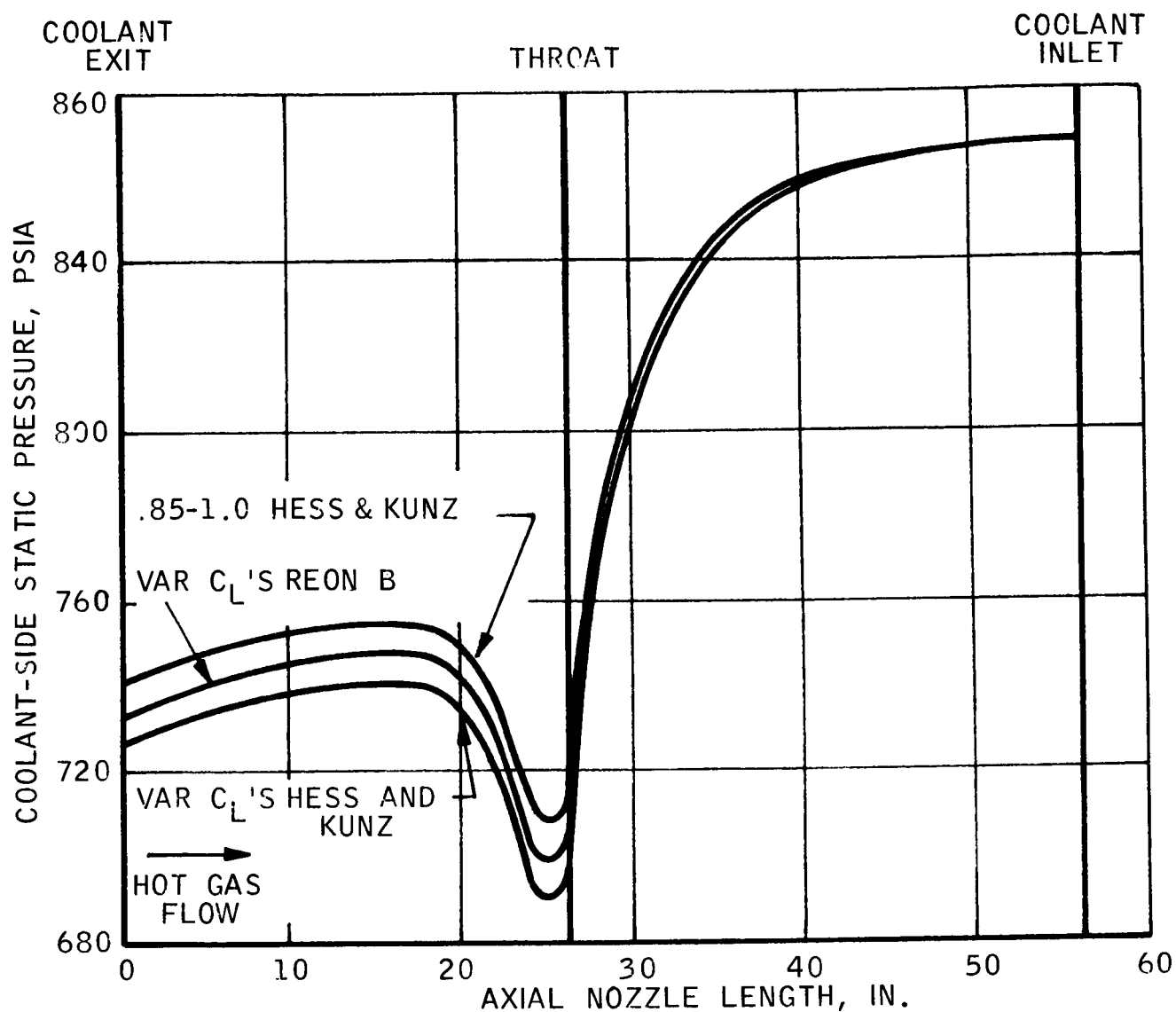


Figure 23

Coolant-Side Static Pressure Profile for
S/N-022 NERVA Nozzle as Predicted by the Nominal Hess and Kunz Design Equation
and the Hess-Kunz and the REON "B" Equations with Variable C_L Values

as a function of axial nozzle length. The 85 to 100% Hess and Kunz prediction and the modified Hess and Kunz equation with variable C_L 's are compared in each of these figures.

The primary effect of the proposed equation in predicting temperature-heat transfer effects is manifested in the coolant-side wall temperature profile as shown in Figure 21. The variable C_L 's result in decreases in the coolant-side wall temperature in the divergent region of the nozzle ranging from 80 to 520°R below the temperature predicted by the 85% Hess and Kunz equation. The change in heat flux is small as are the changes in coolant temperature and static pressure profiles (Figures 22 and 23). As a result of the increase in heat transfer in the skirt region, the bulk temperature rise shown on Figure 22 increased approximately 6 degrees and the overall static pressure (Figure 23) decreased 14 psia, due principally to the increase in the coolant temperature and the corresponding increase in specific volume.

Also shown is a comparison with the recommended bulk temperature equation (the REON "B") with variable C_L 's. The difference between the variable C_L REON "B" coolant temperature and heat flux profiles and the corresponding variable C_L Hess and Kunz predictions were negligible and were not plotted. The predicted coolant-side wall temperature profile, however, was such as to make its comparison of interest. The wall temperature profile based on this equation, when compared with the Hess and Kunz prediction with variable C_L 's, shows a higher axial temperature gradient in both the divergent and convergent regions of the nozzle. The pressure prediction is midway between the values computed for both versions of the Hess and Kunz equation. The predictions are all similar in the throat region.

This comparison of calculated wall temperatures points up the significance of the computational procedure in the prediction of wall temperatures. In the two cases where variable C_L 's were employed with the recommended bulk and film temperature equations, the wall temperature profiles differ significantly, yet the C_L profile basically represents the same data and one is predisposed to infer that the equations could be used interchangeably. However, temperature differences as

high as 200°R are predicted in the convergent region of the nozzle; despite this wall temperature variance, the variation in bulk temperature rise is 1°R (not shown on graph) and the difference in outlet static pressure is only 5.2 psi. The primary difference between the two equations is the magnitude of the thermal gradient in wall temperature in the axial direction.

In connection with the NERVA nozzle S/N-022 tests, a measure of the gas-side wall temperature was attempted by means of braze alloy patches. Partial results (Ref. 23) were obtained by this method as indicated on Figure 24, a plot of the calculated gas-side wall temperatures and the indicated temperature range from the braze alloy data. The braze alloy patches were located in the nozzle at the axial stations noted and were not examined until after the conclusion of the power tests, hence, only the maximum temperature experienced was evidenced by the braze patch appearance. The predicted wall temperature profiles are for the 93.5% power level and should be somewhat below the reported maximums. In general, the braze alloy patches indicate a low wall temperature at the gas exit plane which substantiates the use of the variable C_L 's. The peak in wall temperature at an axial position of 30 inches is not substantiated by the braze patches, nor is the low temperature predicted by the REON "B" equation at an axial distance of 10 to 20 inches.

Due to complexity of nozzle design and the strong dependence of overall heat transfer on the hot-gas-side coefficient, no conclusive comments can be made in this report regarding the applicability of the proposed predictive equations for design or prediction of nozzle test results. A definite recommendation for the optimum design equation can only be made when a coolant-wall temperature is measured directly, preferably, for this nozzle, at a station located in the 30 to 50 in. axial length increment from the coolant exit plane.

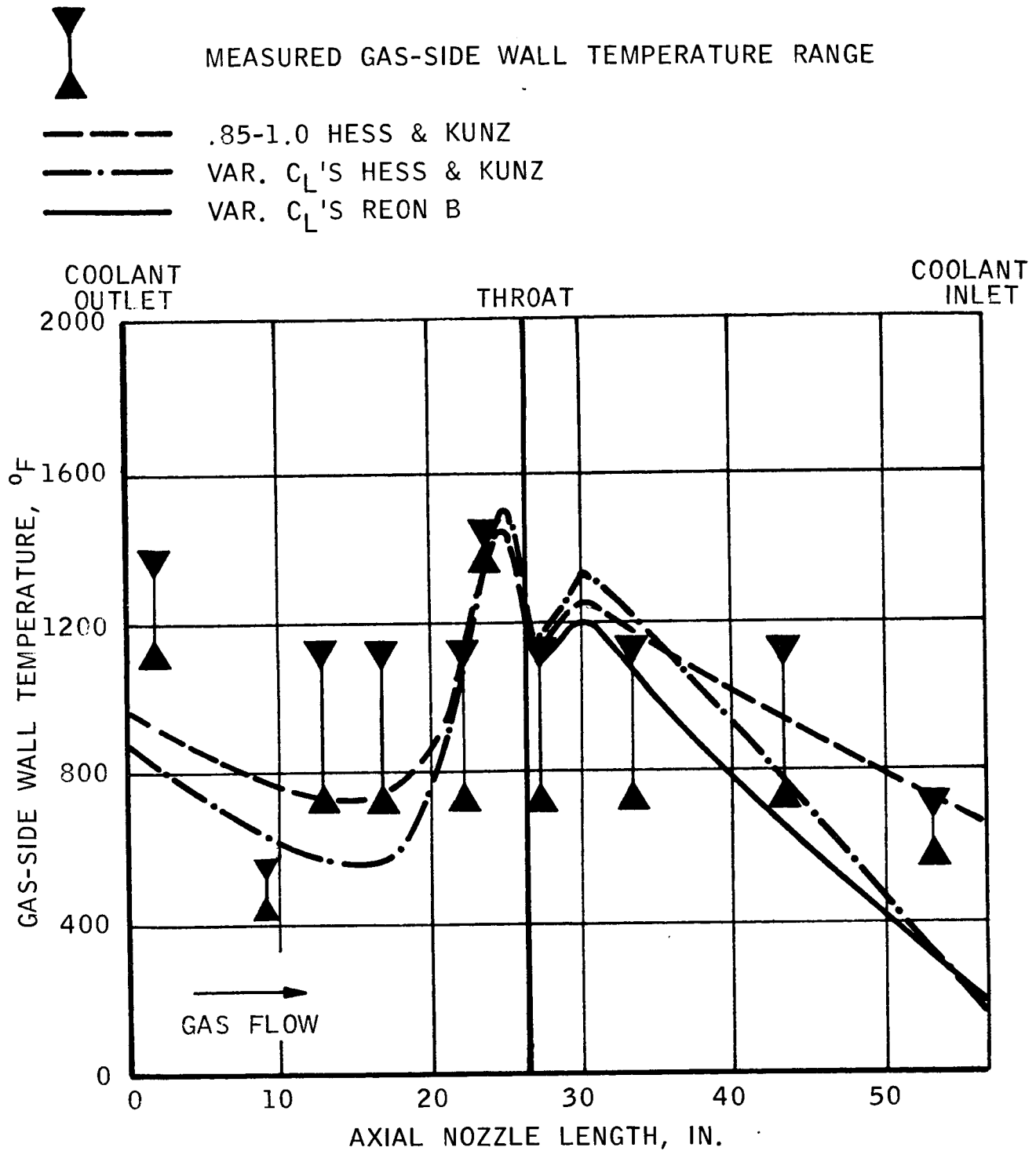


Figure 24

Predicted and Measured Gas-Side Wall Temperature Profile
during Reactor Test NRX-A3

VI. CONCLUSIONS AND RECOMMENDATIONS

An analysis of single-tube heat transfer test data in terms of experimental versus predicted liquid-side coefficients shows no clear evidence of superiority for any one correlating equation. None of the closed-form solutions proposed is satisfactory in representing the data for that portion of the test section in which the wall temperature increases with developed length. An evaluation of the density and scatter of test data points plotted in terms of the ratio of the experimental-to-the-predicted heat transfer coefficient for each equation results in the selection of the Hess and Kunz equation for film-temperature-based correlations and the REON "B" for bulk-temperature-based equations.

The form of this graphical data presentation suggests that a variable liquid-side coefficient, C_L , would better represent the data. The results of incorporating variable C_L values for the two recommended equations were studied in the analysis of NERVA nozzle S/N-022 for a nuclear test firing. A comparison with the nominal design predictions showed that the heat flux profile was hardly changed. The bulk temperature rise and coolant pressure drop were 6.2% higher and 11% lower, respectively, for the variable C_L modification of the 85 to 100% Hess and Kunz design equation. However, predicted coolant-side wall temperatures differed as much as 520°R between the nominal Hess and Kunz design equation and the variable C_L Hess and Kunz and REON "B" equations (with the maximum difference at the coolant inlet plane). Limited braze alloy data for NRX-A3 tend to support this selection.

The Hess and Kunz film-temperature design equation with a variable C_L appears to best represent pertinent single tube test data for cryogenic hydrogen pending development of a model based on a better understanding of energy transfer processes in the fluid. However, direct determination of coolant-side wall temperatures would give us the best indication of which design equation should be used. Such measurements obviously should be made in the region of maximum variation in wall temperatures as predicted by the design equations being compared. For the three equations shown in Figure 21, for example, measurements at axial nozzle lengths of 30 to about 45 in. would be invaluable in selecting the equation which best represents the actual wall temperature profile (for a given gas-side correlation). It is therefore recommended that effort be continued to obtain such measurements.

REFERENCES

1. R. G. Deissler, "Heat Transfer and Fluid Friction for Fully Developed Turbulent Flow of Air and Supercritical Water with Variable Fluid Properties," Trans. ASME, Vol. 76, No. 1, 1954, p. 73.
2. E. J. Szetala, "Heat Transfer to Hydrogen Including Effects of Varying Fluid Properties," ARS Journal, Vol. 32, No. 8, August 1962, p. 1289.
3. H. L. Hess and H. R. Kunz, "A Study of Forced Convection Heat Transfer to Supercritical Hydrogen," J. Heat Transfer (Trans. ASME, Series C), Vol. 87, No. 1, 1965, p. 41.
4. D. A. Wiederecht and G. Sonnemann, "Investigation of the Nonisothermal Friction Factor in the Turbulent Flow of Liquids," ASME Paper No. 60-WA-82, 1960.
5. W. R. Thompson and E. L. Geery, Heat Transfer to Cryogenic Hydrogen at Supercritical Pressures, Aerojet-General Report No. 1842 (AFFTC-TR-61-52), July 1960. Summarized in Advances in Cryogenic Engineering, Vol. 7, Proceedings of the 1961 Cryogenic Engineering Conference, August 15-17, 1961, University of Michigan, Ann Arbor, Paper J-5, p. 391.
6. R. C. Hendricks, R. W. Graham, Y. Y. Hsu, & R. Friedman, Experimental Heat - Transfer Results for Cryogenic Hydrogen Flowing in Tubes at Subcritical and Supercritical Pressures to 800 psia, NASA TN D-3095, March 1966.
7. An Experimental Investigation of Heat Transfer to Hydrogen at Near Critical Temperatures and Supercritical Pressures Flowing Turbulently in Straight and Curved Tubes, REON Report No. 2551, Aerojet-General Corporation, Azusa, California, May 1963.
8. R. C. Hendricks, R. J. Simoneau, and R. F. Friedman, Heat Transfer Characteristics of Cryogenic Hydrogen from 1000 to 2500 psia Flowing Upward in Uniformly Heated Straight Tubes, NASA TN D-2977, September 1965.
9. J. R. McCarthy and H. Wolf, Heat Transfer Characteristics of Gaseous Hydrogen and Helium, Research Report 60-12, Rocketdyne, North American Aviation, Inc., December 1960.
10. M. Dalle Donne and F. W. Bowditch, "High Temperature Heat Transfer," Nuclear Eng., Vol. 8, No. 8C, January 1963, p. 20.
11. Interim internally-generated design equation, Aerojet-General Corporation (unpublished).
12. W. S. Miller, J. D. Seader, and D. M. Trebes, "Forced Convection Heat Transfer to Liquid Hydrogen at Supercritical Pressures," Rocketdyne, North American Aviation, Inc. Paper presented at the International Institute of Refrigeration, Commission I, Grenoble, France, June 9-11, 1965.

13. W. H. McAdams, Heat Transmission, McGraw-Hill Book Company, Inc., New York, N.Y., third edition, 1954, p. 226.
14. E. N. Sieder and G. E. Tate, "Heat Transfer and Pressure Drop of Liquids in Tubes," Ind. Eng. Chem., Vol. 28, 1936, p. 1429.
15. R. D. Wood, Heat Transfer in the Critical Region: Experimental Investigation of Radial Temperature and Velocity Profiles, Ph.D. Dissertation, Northwestern University, Evanston Illinois, June 1963.
16. K. Goldmann, "Heat Transfer to Supercritical Water and Other Fluids with Temperature Dependent Properties," Chem. Eng. Prog. Symp. Series 50, No. 11, 1954, p. 105.
17. J. V. Miller and M. F. Taylor, Improved Method of Predicting Surface Temperatures in Hydrogen-Cooled Nuclear Rocket Reactor at High Surface-to-Bulk Temperature Ratios, NASA TN-D-2594, January 1965.
18. K. D. Williamson, Jr., and J. R. Bartlit, "Forced Convection Heat Transfer to Flowing Hydrogen, 60-500°R," Los Alamos Scientific Laboratory, Univ. of California (unpublished).
19. H. Ito, "Friction Factors for Turbulent Flow in Curved Pipes," J. Basic Engineering (Trans. ASME, Series D), Vol. 81, 1959, p. 123.
20. W. H. McAdams, loc. cit., p. 228.
21. R. A. Seban and E. F. McLaughlin, "Heat Transfer in Tube Coils with Laminar and Turbulent Flow," Int. J. of Heat Transfer, Vol. 6, 1963, p. 387.
22. R. C. Hendricks and F. F. Simon, "Heat Transfer to Hydrogen Flowing in a Curved Tube," Proc. Multi-Phase Flow Symposium, N. J. Lipstein, ed., ASME, 1963, p. 90.
23. Unpublished NRX-A3 Nozzle test results report (REON Report RN-S-0249).



AEROJET-GENERAL CORPORATION